Energy Recovery from Waste Tires Via Thermochemical Pathways

Kiran R. G. Burra, Zhiwei Wang, Matteo Policella, and Ashwani K. Gupta

Abstract Demand for automotive tires has been increasing at a significant rate to reach production rate of 2.9 billion in 2017 that contributed to the generation of almost 1 billion waste tires. The pathways for handling of these waste tires have been limited to aggregate construction applications and direct incineration as fuel. The rate of recycling feasibility was limited by the availability of waste tires with structure intact for their upgrading and reuse in the economy. In the USA, although 40% of the waste tires are disposed by combustion for energy recovery in cement kilns, pulp and paper mills, and electricity generation, the presence of sulfur from vulcanized rubber, the production of hazardous pollutants, and low temperatures caused due to slow heterogenous combustion leads to significant energy and resource losses. Additionally, this pathway is limited to thermal energy production and thus lacks versatility. Alternative thermochemical pathways such as pyrolysis and gasification offer better pathways for the utilization of these wastes as they provide uniform products such as synthetic gas, bio-oil and char. Versatility is also achieved via syngas production as it is a precursor to liquid fuels and various other essential petrochemicals. These pathways provide improved energy efficiency, feasibility, and scalability for increased waste tire utilization and value outcome compared to the current application pathways. Results are reported from the investigations on high-temperature pyrolysis and CO_2-assisted gasification of waste tires with focus on the evolutionary behavior of syngas production, its constituents, and energy yield in lab-scale fixed-bed reactor. The impact of CO_2 addition, temperature, and the addition of biomass feedstock to the waste tire was investigated to understand the feasibility of waste tire disposal via this pathway while also utilizing the CO_2 pollutant and maintaining high energy efficiency. Lack of inhibitive effects observed when tire was co-processed with biomass, makes the disposal of waste tires along with other

K. R. G. Burra · Z. Wang · M. Policella · A. K. Gupta (✉)
Department of Mechanical Engineering, The Combustion Laboratory, University of Maryland, College Park, MD 20742, USA
e-mail: akgupta@umd.edu

Z. Wang
College of Environmental Engineering, Henan University of Technology, Zhengzhou 450001, PR, China

A. Gupta et al. (eds.), *Advances in Energy and Combustion*, Green Energy and Technology,
https://doi.org/10.1007/978-981-16-2648-7_21

wastes easier along with established feasibility regime for efficient and economical disposal of waste tires while recovering energy and utilizing CO_2.

Keywords Waste tires · Syngas · Gasification · Pyrolysis · Recycling · Energy recovery

Nomenclature

α	Extent of mass-loss conversion
BET	Brunauer–Emmett–Teller
BR	Butadiene rubber
$\text{Energy}_{\text{input}}$	Electrical energy consumed by furnaces
GC-TCD	Gas chromatography-thermal conductivity detector
LHV	Low-heating value
M_i	Mass flow rate of species 'i'
$\text{m}_{\text{feedstock}}$	Initial mass of the feedstock in the lab-scale reactor
m_{syngas}	Cumulated mass of syngas
$M(T)$	Mass of sample left in the TGA at temperature 'T'
NR	Natural rubber
OEE	Overall energy efficiency
PET	Polyethylene terephthalate
ρ_i	Density of species 'i' at GC inlet
SBR	Styrene–butadiene rubber
T	Temperature
TDF	Tire-derived fuel
TGA	Thermogravimetric analysis
V_i	Volumetric flow rate
X_i	Mole fraction of species 'i' recorded by the GC

1 Introduction

With the growing penetration of automobiles in the marketplace, their sustainability is dependent on the availability and management of the fuel, and its materials. The increased utilization of fossil fuels in transportation sector and industry is leading to lack of fuel availability and increase in global warming from the imbalance between carbon emissions and its sequestration. This can be seen by the trend of CO_2 concentration in the atmosphere which reached 415 ppm in 2020 from ~280 ppm in the pre-industrial era [1]. Several efforts are being made here to support CO_2 management and control in the transportation sector with increased penetration of electric vehicles and light-duty trucks. California has promulgated 100% electric vehicle

sales by 2035 and phase out of gasoline powered vehicles by 2045. While renewable alternatives and carbon-free transportation are still in developing phase, their scalability and penetration to completely replace the carbon-based infrastructure are questionable. These resources need to be supplemented with carbonaceous fossil fuel resources for the foreseeable future to achieve sustainable energy while seeking carbon neutral footprint. All electric vehicles are justifiable only with the electricity produced from renewable sources.

In addition to the fuel crisis, the handling and disposal of waste tires created by increases in the automotive sector poses significant challenge to sustainably continue producing or recovering these tires. An estimated 2.9 billion automobile tires were produced in 2017, while almost 1 billion waste tires were generated [3]. Predictions based on the current demand growth in automotive sector of 4.1% are expected to result in production of almost 3.2 billion tires by 2022 [4]. Such a rapid growth with the current trends of recovery will be unsustainable. In the USA alone, 255 million waste tires were disposed in 2017, wherein 15% were landfilled, and 41% were combusted for energy recovery [2]. Figure 1 reveals the statistics in 2017 and the current modes of utilization of waste tires which account for 81.4% going to the market while 15% landfilled and the rest remained unaccounted [2]. Tire-derived fuel (TDF) accounts for 41% of the utilization. Other sectors include cement kilns (19%), pulp and paper mills (12%), and electric utilities (10%) for the energy recovered. Almost 30% of this waste tires are ground for use in applications that included asphalt for roads, sport surfaces and mulch, and extrusion/molded products. Utilization in construction offers lower-value applications compared to other applications. The

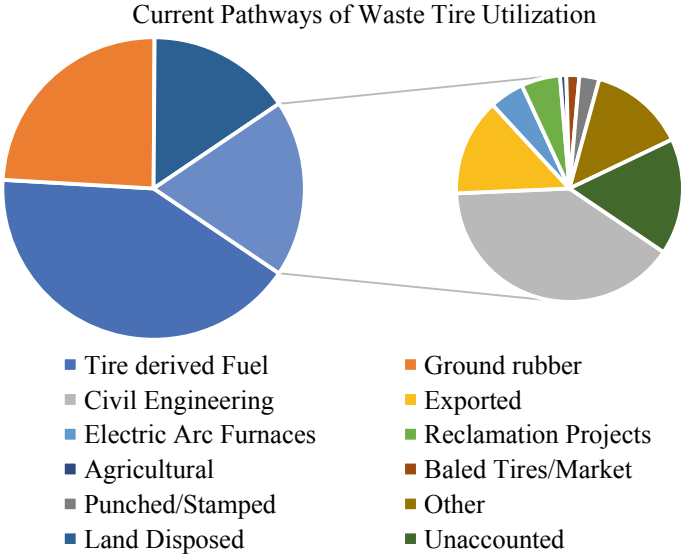

Fig. 1 Fate of waste tires in the USA in 2017 [2]. [Color codes are does not account for all the colors used]

infrastructure that accounted for in TDF includes fossil fuel equivalent combustion units where the waste tire is possibly mixed with other fuels such as coal, and biomass for energy recovery. While these pathways operate with solid fuel efficiencies which is lower than gas-phase combustion due to lower temperatures attained, they also pose environmental hazard in terms of emissions of polychlorinated dibenzodioxins, Zn, SO_x from high S content in vulcanized rubber, polyaromatic hydrocarbons, particulates, odors and other toxic emissions [5]. Thus, to operate in low-environmental impact mode regulated by the government, it requires multi-stage flue-gas cleaning, which significantly lowers the net efficiency of the waste tire utility and recuperated energy.

These statistics reveal the need for alternative pathways for waste tire disposal, especially for energy purposes with the consideration of the imminent fuel crisis and rapidly increasing CO_2 concentration in the environment. Thermochemical pathways such as pyrolysis and gasification for oil and syngas yields provide significant advantages in this aspect of feedstock utilization. Pyrolysis involves thermal decomposition of carbonaceous feedstocks at high temperature to form syngas, oil and char products [6]. Depending on the desired product phase, the operating conditions are modified. High heating rates and low vapor residence times are used when oil is desired, while low heating rates and high residence times are used for increased char residue, and high temperatures above 700 °C when syngas is desired. In the case of gasification, the sample is thermally decomposed at temperatures above 750 °C in the presence of a mild oxidizing/gasifying agent such as H_2O, CO_2, diluted O_2/air to yield significantly high syngas compared to pyrolysis [6]. While temperature has a crucial role in the yield of syngas, its composition is significantly controlled by the gasifying agent where steam (H_2O) yields H_2-rich syngas, CO_2 yields CO-rich syngas, and air/O_2 is used for autothermal operation. Although these processes are endothermic, the reformed uniform syngas, which is the focus of this chapter, is of high quality in terms of its compositional uniformity, heating value, yield, energy recovery and capability to modify composition with minimal downstream resources, via water–gas shift reaction. Additionally, the versatility in applications offered by syngas is unparalleled, because various pathways have been extensively studied and implemented industrially such as Fischer–Tropsch synthesis for liquid fuels from syngas [6]. Significant literature is available on the utilization of these pathways for waste tire conversion, and some of it will be discussed in the context of evolutionary behavior and energetic feasibility later in this chapter to establish the knowledge and its gap compared to the available studies [3–5, 7–29]. This will be preceded by understanding of waste tire constituents, composition and their behavior in the context of thermochemical conversion.

2 Characterization of the Waste Tires

To characterize waste tires' feedstock, we need to initially investigate the composition and its variability in the waste tires collected. Typically, tires consist of a blend of

natural (NR) and synthetic rubber (SR) wherein polybutadiene rubber (BR) and styrene–butadiene rubber (SBR) are the most common examples of SR [30]. Carbon black is added to this blend for enhanced resistance against abrasion, in addition to extracting heat from the tread and the belt. For reinforcement, steel wires/textile fabrics (polyester, rayon and nylon cords) are incorporated into this rubber mix for enhancing strength and durability of tires [23]. During the vulcanization of the rubber constituents, ZnO is added to control and improve its physical properties, while sulfur is added as cross-linking agent between the elastomer chains while hardening the final product and improving its resistance against thermal deformation at high temperatures. While these are the major components, additional trace compounds are also added to improve their quality and manufacturing, such as a mix of aromatic hydrocarbons called extender oils and resins as plasticizers for improved shaping and molding, antioxidants and antiozonants to combat oxidization and ozone influence [5]. Different sources, i.e., different automobiles classes, have their specific needs and thus, the characteristics of the tires utilized are also modified in terms of the elastomers' composition, reinforcement and its material, treading, geometry, carbon black and other additives. For example, while passenger car tires are composed of 35% natural rubber (NR) and 65% polybutadiene rubber (BR), truck tires contain 51% NR, 10% BR and 39% styrene–butadiene rubber (SBR) [2]. Table 1 provides further differentiation on the composition of typical passenger car and truck tires. Literature also provides proximate and ultimate analysis of waste tires varying in their sources and properties, and they are summarized in Table 2 [5]. This table reveals the significance of waste tires in terms of the calorific value of this feedstock that is seen more than 30–35 MJ/kg with some as high as 40 MJ/kg. These heating values

Table 1 Typical constituents and composition of waste tire and their utility [14, 30]

Component	Passenger tire (wt. %)	Truck tire (wt. %)	Comments/examples
Rubber	47	45	Synthetic and natural rubbers, examples: styrene–butadiene rubber, natural rubber (polyisoprene), nitrile rubber, chloroprene rubber, polybutadiene rubber
Carbon black	21.5	22	Added to strengthen the rubber and help in abrasive resistance
Metal	16.5	21.5	Steel belts and chords for strength
Textile	5.5	–	Reinforcement
Zinc oxide	1	2	Used with stearic acid to control vulcanization and enhance physical properties of rubber
Sulfur	1	1	Used to control rubber polymer chains, harden and prevent excessive deformation at high temperatures
Additives	7.5	5	Example: Clay/silica as a partial replacement to carbon black

Table 2 Proximate and ultimate analysis of various waste tires and their calorific value [5]

Elemental analysis (wt. % dry basis)						Proximate analysis (wt. % as received basis)				Calorific value (MJ/kg)	References
C	H	N	S	O	Ash	Ash	Volatiles	Fixed carbon	Moisture		
81.72	6.54	0.55	1.87	2.68	6.64	6.64	62.58	30.07	0.71	nr	[31]
83.8	6.9	0.6	2	2.3	4.4	4.3	63.4	30.4	1.9	nr	[32]
83.8	7.6	0.4	1.4	3.1	3.7	3.7	67.3	28.5	0.5	36.45	[33]
82.36	6.92	2.3	1.4	2.03	5	4.95	73.74	20.22	1.09	37.06	[25]
75.5	6.75	0.81	1.44	15.5	+	20.1	57.5	20.85	1.53	29.18	[21]
85.9	8	0.4	1	2.3	2.4	2.4	66.5	30.3	0.8	40	[19]
75.4	7.03	0.21	1.62	5.09	10.21	10.21	62.32	26.26	1.31	33.29	[34]
84.33	7.81	0.49	1.66	3.32	2.4	7.1	62.2	29.4	1.3	40	[12]
82.8	7.6	0.5	1.3	4.5	3.3	3.3	68.7	27.2	0.8	36.46	[35]
86.7	8.1	0.4	1.4	1.3	2.1	8	61.9	29.5	0.7	36.2	[8]
80.29	7.25	0.31	1.84	4.9	5.41	5.3	67.5	25.2	2.1	37.3	[36]
85.05	6.79	0.5	1.53	1.75	4.4	4.35	62.24	32.28	1.14	34.9	[37]
81.5	7.1	0.5	1.4	3.4	6.1	6.07	64.87	28.56	0.5	36.8	[38]
86.09	6.74	0.19	1.93	1.35	3.7	3.7	65.5	29.4	0.9	nr	[26]
86.7	6.9	0.3	1.9	0.9	3.3	4.4	64	30.7	0.9	31.8	[39]
83.92	6.83	0.78	0.92	3.39	4.16	4.16	64.97	30.08	0.75	38.6	[40]
85.25	7.94	0.41	1.38	1.19	3.83	3.83	64.09	31.14	0.94	nr	[41]
83	6.79	0.32	1.37	3.46	5.06	5	64.1	29.7	1.2	35	[42]
67.08	6.12	0.17	2.05	24.58	+	19.1	59.69	19.45	1.72	27.37	[11]
81.79	7.99	0.48	1.81	3.04	4.9	4.88	65.74	28.98	0.4	38.3	[43]

(continued)

Table 2 (continued)

Elemental analysis (wt. % dry basis)						Proximate analysis (wt. % as received basis)				Calorific value (MJ/kg)	References
C	H	N	S	O	Ash	Ash	Volatiles	Fixed carbon	Moisture		
84	7.19	0.49	1.42	3.3	3.6	3.6	65.6	30	0.8	38.8	[44]
83.15	6.78	0.28	1.77	0.84	7.1	7.1	61.9	29.9	1.1	37.35	[45]
74.3	7.2	0.9	1.71	15.89	+	18.9	58.2	21.3	1.6	30.5	[17]

are comparable to some of the high-quality fuels such as anthracite and bituminous coals, and biofuels such as alcohol fuels, but lower than domestic and transportation fuels such as gasoline, kerosene and methane which are higher than 42–45 MJ/kg. Table 2 also reveals significantly high carbon content and fixed carbon in the waste tires which reveals high quality of the feedstock and emphasizes the importance of carbon black's presence in the context of its conversion as this means high levels of char residue from pyrolysis. By extension, it also means that if gasified, major reactions responsible for mass conversion are heterogenous reaction of the fixed carbon components with the gasifying agent. This reveals the potential of waste tires for use as an ideal source of energy and for coal replacement applications.

So, for the context of understanding the feasibility of waste tires, we restrict our discussions in this chapter to specific types of tires in terms of the vehicle class. From the statistics of 2017 given in Table 3, significant portions (almost 73%) of waste tires are from passenger car, while commercial truck and bus tires account for up to 11.4% of the total waste tires collected [2]. With this table as the basis, we restricted our experimental investigation to passenger vehicle waste tire. Further details of our materials and methods and observations will be preceded by various results available in the literature regarding pyrolyzing and gasifying waste tires for syngas production.

Table 3 Types of tires disposed in the USA in 2017 [2]

Tire class	Millions of Tires	Market %	Average weight (kg)	Weight (1000 × tons)
Light-duty tires	**254.6**	**88.6**	**10.2**	**2864.3**
Passenger tire replacements	209.7	73.0		
Light truck tire replacements	31.3	10.9		
Tires from scrapped vehicles	13.6	4.7		
Commercial tires	**32.7**	**11.4**	**54.4**	**1962.0**
Medium, wide-base, heavy truck replacement tires	19.7	6.9		
Tires from scrapped trucks and buses	13.0	4.5		
Total tires hauled	**287.3**	**100.0**	**15.24**	**4826.3**
Used tires culled	**37.9**	**13.2**	**15.24**	**637.1**
Net scrap tires	**249.4**			**4189.2**

3 Thermochemical Conversion of Waste Tires

Various types of processes were proposed and investigated to convert waste tires for energy, fuels or chemicals recovery. Significant portion of the waste tire pyrolysis had been vested in the production of oil, possibly via fast pyrolysis. Literature also provides us with a compiled comparison of the state of the art of pyrolysis of waste tires from different studies in several review articles [5, 14, 16]. Thus, we limit the scope of this chapter, in the context of pyrolysis results reported in the literature, to the results compiled from these review articles and their findings. Table 4 provides us with a comparison of various pyrolysis studies reported and reveals the relative yield of oil, char and gas products [14]. From this table, one can see that the char yield was around 30–50% (by wt.), depending on the reactor conditions used. Such a yield of char is significantly high that is limited to the processes designed for oil production. This is a result of the high carbon black and thus fixed carbon content, which is a characteristic of the waste tire feedstock. Additionally, Table 5 provides information on the quality of oil produced in comparison with petrochemical fuels. This reveals the requirement of downstream catalytic refining of the oil, possibly novel hydrogenation, to make it compatible for fuel applications, especially in terms modifying the flash point, calorific value enhancement, particulate and carbon residue removal, and improving the boiling point characteristics [14]. The requirement of significant refining adds to the issue of high char yields which leads to an end-result of relatively low yields of the final fuel products. The high char yield, unwanted high gas yield and catalytic refining requirements currently limit the capability of pyrolysis as a pathway for the purposes of oil/liquid fuel production.

To alleviate these issues, various strategies have been proposed. As the gas yield from this pyrolysis for liquid process is in the range of around 2–25% (by wt.), valuable utilization of this by-product is essential to support the overall process. The high char yield from pyrolysis still makes this process less attractive and calls for another strategy to target both the issues on high gas and less char yields. Gasification is proposed to avoid direct formation of liquid yield and reform all the intermediates from waste tires into syngas rich in H_2, CO, CH_4, impurities of C_2 and C_3 hydrocarbons and CO_2. This not only improves the effective yield of the desired product to above 70% (by wt.), but also provides uniform and versatile syngas, which can be used for various applications. Even modifying pyrolysis to focus on gas yield, such as high temperature mesh reactor tests shown in Table 4 reveals the gas yield to be higher than 70% (by wt.) and minimized char yield to fixed carbon content levels.

Significant knowledge is available on gasification of waste tires involving various reactor systems, operating conditions and gasifying agents, and they are summarized in some of the well-compiled review articles in the literature [16]. To obtain a complete picture on the gasification of waste tires, one needs to first investigate pyrolysis under similar conditions as this is the first inherent step in gasification. Conesa et al. found from pyrolysis of waste with high vapor residence times (>10 min) that the increase in temperature from 450 to 1000 °C, changed the char yield from 35 to 37% due to the high residence time, while the gas yield increased from 27 to 62%

Table 4 Summary of different pyrolysis tests on waste tires and their relative product yields [14]

Reactor	Experimental conditions	Maximum oil yield				References
		T (°C)	Oil (wt.%)	Char (wt.%)	Gas (wt.%)	
Fixed bed, batch	400–700 °C	500	40.26	47.88	11.86	[46]
Fixed bed, batch	500–1000 °C, 1200 °C/min	500	58	37	5	[36]
Fixed bed, batch	300–720 °C, 5–80 °C/min, 50 g	720	58.8	26.4	14.8	[19]
Fixed bed, batch	450–600 °C, 5 °C/min, 3 kg	475	58.2	37.3	4.5	[12]
Fixed bed, batch	950 °C, ~2 °C/min, 1000 kg	950	20.9	40.7	23.9	[47]
Fixed bed, batch	350–600 °C, 5 & 35 °C/min,	400	38.8	34	27.2	[10]
Fixed bed, batch	300–700 °C, 15 °C/min, 175 g	700	38.5	43.7	17.8	[48]
Fixed bed, batch	375–500 °C, 10 °C/min, 10 g	425	60	~30	~10	[11]
Fixed bed, batch, internal fire tubes	375–575 °C, 750 g	475	55	36	9	[49]
Fixed, wire mesh, fast reactor	390–890 °C, 70–90 °C/s	860	~5	~22	~73	[29]
Moving screw bed	600–800 °C, 3.5–8 kg/h throughput	600	48.4	39.9	11.7	[31]
Rotary kiln	550–680 °C, 4.8 kg/h	550	38.12	49.09	2.39	[50]
Rotary kiln	450–650 °C, 12–15 kg/h	500	45.1	41.3	13.6	[37]
Fluidized bed	740 °C, 1 kg/h	740	30.2	48.5	20.9	[51]
Fluidized bed	750–780 °C, 30 kg/h	750	31.9	38	28.5	[51]
Fluidized bed	700 °C, 200 kg/h	700	26.8	35.8	19	[51]
Fluidized bed	450–600 °C, ~220 kg/h	450	55	42.5	2.5	[52]
Circulating fluidized bed	360–810 °C, 5 kg/h	450	~52	~28	~15	[35]
Conical spouted bed	425 and 500 °C	500	~62	~35	~3	[53]

(continued)

Table 4 (continued)

Reactor	Experimental conditions	Maximum oil yield				References
		T (°C)	Oil (wt.%)	Char (wt.%)	Gas (wt.%)	
Vacuum, conical spouted bed	425 and 500 °C, 25 & 50 kPa	500	~60	~34	~4	[54]
Vacuum	485–550 °C, batch (80–180 kg) and continuous	520	45	36	6	[55]
Vacuum	500 °C, pilot-scale semi-continuous	500	56.5	33.4	10.1	[56]
Vacuum	450–600 °C, 100 g batch	550	47.1	36.9	16	[40]
Closed batch reactor	350–450 °C, 30 °C/min	450	~63	~30	~7	[57]
Drop tube reactor	450–1000 °C, 30 g/h	450	37.8	35.3	26.9	[26]

at the expense of oil yield that decreased from 38% to negligible levels [26]. This is because of high-temperature operation leads to enhanced secondary reactions such as thermal cracking of the hydrocarbon intermediates to form light hydrocarbons, H_2, CO and CO_2 at significant vapor residence times. These results are also evident from the data shown in Tables 6 [14]. From Table 4, one can see that high heating rates (70–90 K/s), high temperature and vapor residence times (15 min) in a wire-mesh microreactor led to significantly high gas yield of 73% [29]. But at temperatures of 450–600 °C with short residence times (~2 min), heating rate of 5 °C/min led to maximum oil yield of 58%. These results also showed that temperature had minimal effect on the relative yields. Although significant literature is available on pyrolytic breakdown of waste tires, focus on syngas yield and evolutionary behavior during gasification is still lacking. Our studies into high-temperature pyrolysis of waste tires and its mixtures with biomass provide comprehensive information (given in the following sections) that establishes the feasibility of syngas recovery from waste tires.

Various reactor systems have been utilized for the gasification of waste tires, which included fixed bed, bubbling and circulating fluidized bed reactors of both lab-scale and pilot-scale, rotary-kiln reactors and plasma gasifiers [5, 16]. Knowledge on the gasification at pilot scale has been limited to using air and steam as the gasifying agent. The addition of air oxidized some of the inflammable components evolved from waste tire decomposition while the exothermic reaction from this oxidation supports the endothermic decomposition reactions responsible for volatile evolution. This leads to syngas with relatively high CO_2 compared to other gasifying agents but provided with the advantage of autothermal operation, i.e., alleviation of the need of external heat/energy source for continuous operation and maintaining the desired temperature. Due to the ease of energy transfer and its similarity to incineration,

Table 5 Properties of oil products obtained from waste tire pyrolysis in the literature [14]

Property	Ref. [47]	[37]	[10]	[58]	Kerosene [59]	Gas oil	Light fuel oil
Flash point (°C)	20	17	65	43	40	75	79
Carbon residue (%)	2.2	1.78	–	–	–	< 0.35	–
Density ($kg.l^{-1}$)	0.91	0.962	0.833	0.924	0.84	0.78	0.89
Viscosity (cSt at 40 °C)	6.3	–	–	3.77	1.2	3.3	21
Viscosity (cSt at 50 °C)	–	2.44	1.01	0.924	–	–	–
Viscosity (cSt at 60 °C)	2.38	–	–	–	–	–	–
Carbon (wt.%)	88.0	84.26	79.61	–	–	87.1	85.5
Hydrogen (wt.%)	9.4	10.39	10.04	–	13.6	12.8	12.4
Nitrogen (wt.%)	0.45	0.42	0.94	–	–	0.05	0.15
Sulfur (wt.%)	1.5	1.54	0.11	0.72	0.1	0.9	1.4
Oxygen (wt.%)	0.5	3.39	9.3	–	–	–	–
Initial B.Pt (°C)	100	–	38.5	70	140	180	200
10% B.Pt (°C)	140	–	58.2	114.5	–	–	–
50% B.Pt (°C)	264	–	174.8	296.1	200	300	347
90% B.Pt (°C)	355	–	–	386.4	315	–	–
Calorific value (MJ/kg)	42	41.7	42.66	38	46.6	46	44.8
Ash (wt.%)	0.002	Trace	–	0.31	–	0.01	0.02
Moisture (vol.%)	4.6	0.88 (wt.%)	–	–	–	0.05	0.1

autothermal mode is the most preferred way of gasification currently used at large scale at the expense of syngas quality [3]. A novel pathway of pilot-scale solar air gasification was reported in Wieckert et al. concerning the conversion of waste tires in comparison with various other feedstocks including coal that reported sustainable energy efficiency of 27% in waste tire conversion [60]. While solar concentrator supported gasification has significant potential in waste tire conversion, the lack of knowledge and the challenges associated with energy losses in the current solar

Table 6 Proximate and ultimate analysis, and calorific value of the tested feedstocks [4]

Sample	Volatile (wt.%)	Fixed carbon (wt.%)	Ash (wt.%)	Moisture (wt.%)	LHV (MJ kg^{-1})	Carbon (wt.%)	Hydrogen (wt.%)	Nitrogen (wt.%)	Oxygen (wt.%)	Sulfur (wt.%)
Waste tire	62.5	27.9	8.9	0.7	33.3	81.85	6.66	1.7	9.8	1.37
Pine bark	63.9	26.2	4.8	5.2	18.8	50.37	4.20	1.61	43.81	0.03

concentrator reactors limit this pathway but is a pursuable challenge for carbon neutral production of energy/chemicals from waste tires and other wastes.

Increase in temperature was found to increase the syngas yield and thus the energy recovery ratio (syngas energy/waste tire energy) as found by Raman et al. who reported the energy recovery ratio improved linearly from 0.1 to 0.4 with increase in temperature from 900 to 1060 K [61]. Other studies have found 0.4 for the highest energy recovery obtained under these conditions of air gasification. In the case of steam gasification, Donatelli et al. found that increase in steam/feedstock ratio decreased the calorific content of the syngas (possibly by reforming all the hydrocarbons into H_2 and CO) to result in decreased energy recovery ratio [20, 62]. Various gasifying agents were investigated to convert waste tires including air, steam, and CO_2 but studies on CO_2 gasification are visibly limited [16]. While air gasification provides autothermal operation and steam gasification provides high H_2 yield, the advantages of CO_2 gasification are multi-fold and more eco-friendly. Incorporation of CO_2 into waste tire gasification leads to utilization of CO_2 for char gasification and volatiles reforming which results in syngas enhancement and improved carbon conversion. It also assists in net conversion of CO_2 into valuable syngas which leads toward making this process more carbon neutral. High-temperature CO_2 is available as flue gas in some industries, such as coal combustion plants, which can be synergistically used for waste tire conversion for effective carbon utilization. Further studies into the scope of CO_2 gasification with respect to waste tire conversion are necessary, and lab-scale studies have been carried out by our group in this direction that support effective and efficient conversion of waste tires using CO_2. Following sections provide detailed experimental setup and result that established feasibility of CO_2-assisted gasification of waste tires as a sustainable pathway for waste tire conversion.

The influence of catalyst in waste tire conversion was conducted using dolomite addition that resulted in lowered calorific value of syngas, and thus the energy recovery ratio. However, the utilization of transition metal (Ni, Co, Fe, Cu) supported on Al_2O_3 carried out by Zhang et al. reported the formation of carbon nanotubes in the char yield that constituted to 8–12 wt.% of the char [63]. Studies on the comparison of commercial Ni-based catalysts, with mineral catalysts such as dolomite and olivine, were also reported in the literature using bubbling fluidized bed gasifier. These studies showed improved H_2 and syngas yield via reforming/cracking reactions at the expense of calorific output. The issues of catalyst deactivation from coke deposition were as expected due to high levels of char formation tendency and hydrocarbon presence with Ni/Al_2O_3 leading to H-abstraction and enhanced H_2 yield from 24 to 57%. Utilization of this carbon deposition for the production of carbon nanotubes was also investigated [63]. Further studies into such a pathway of H_2 and carbon nanotubes are essential to establish its feasibility and operating conditions for optimal products as control over the quality of carbon nanotubes, and their extraction is critical to establish their production. Syngas with H_2 content as high as 99% was also produced from the gasification of waste tires in the presence of CaO [64]. Although the review article claims CaO to be catalyst, H_2 enhancement was carried out via well-known sorption enhanced reforming to remove CO_2 via carbonization of

CaO into $CaCO_3$ which can drive the product equilibrium to high H_2 partial pressures [16]. But the reusability of CaO was low, and thus the state-of-the-art feasibility is questionable as reported in gasification and sorption-enhanced reforming studies in the literature.

The gasification of waste tires with other feedstocks including coal products such as lignite, biomass/biowaste such as pinewood, palm kernel shells, municipal sludge, olive husk, almond shells, palm fruit and plastic wastes such as polyethylene terephthalate (PET) from plastic bottles, and their mixtures were also carried out for various selected goals [16]. Almond shells and palm fruits were added to improve the char reactivity from an otherwise stable low-reactive tire char and found significant improvement in carbon conversion levels via co-conversion. Even in the cases of co-processing, although the values of syngas yield, quality and energy with respect to temperature, catalyst and feedstock ratio were carried out, systematic studies into the impact of feedstock composition and the feedstock ratio on the syngas components and conversion behavior, especially the understanding of possible nonlinear synergy is still lacking in the literature. Enhanced syngas evolution via nonlinear interaction between polymer wastes and biomass/coal were reported with selected plastics but such studies involving waste tires are still lacking [65–70]. Studies to understand the impact of co-processing waste tire with biomass via pyrolysis and gasification have also been carried out and reported in the following sections [4, 15, 18].

4 Methods and Materials

4.1 Feedstock Materials

For studies to establish the feasibility of waste tire conversion via thermochemical pathways, we utilized used-passenger car tire as such waste constitutes to almost 90% of the total waste tires collected in the USA [2]. The waste tire used was a Goodyear winter radial tire reinforced with textile fibers instead of metal wires. For lab-scale pyrolysis and gasification studies, this tire was cut into small cubes having each side of approx. 1.5–2 cm. Thermogravimetric studies were also carried out to characterize this feedstock, and for such microscale studies, the waste tire was frozen using liquid N_2 and then grounded with rubber particles of approx. ~100 μmin size. For each case, the total tested feedstock of waste tire included a mix of 60 wt.% from the tire tread and 40 wt.% from the side wall. Due to reinforcement and tire construction, the composition of the waste tire varied from the side wall to tread. This proportional mixture was utilized to accurately represent a real waste tire.

For co-pyrolysis and co-gasification studies, pine bark was chosen as a representative forestry residue biomass feedstock that was added to the waste tire. The pine bark feedstock was obtained from a local nursery, and the acquired feedstock was dried at 105 °C for 24 h to minimize moisture content before blending with the waste

tire. The samples acquired were characterized using proximate and ultimate analysis to establish the fixed carbon and volatile content along with carbon, hydrogen, nitrogen and sulfur (CHNS) content of the chosen feedstocks. Thermogravimetric analysis (TGA) was utilized following modified ASTM 7582–15 standard for proximate analysis, while low heating value (LHV) of the samples and the pyrolysis of char blends was obtained using rapid screening device (5E-KCIII, China); see Table 6 for these results.

4.2 Thermogravimetric Analysis (TGA)

Thermogravimetric analysis was carried out using TA Instruments SDT Q600 with each sample weighing approximately 1–3 mg. The TGA was equipped with horizontal beam balance in an electric furnace and was capable of operating at temperatures of up to 1500 °C. The samples of waste tire and pine bark were ground to 140 mesh particle size separately and as blends for these analyses. The samples were heated from room temperature to 100 °C and maintained for 10 min to remove moisture, followed by heating the sample at 10 or 20 °C/min to reach to temperatures of 950 °C in the presence of high-purity Ar at 100 ml/min. During this heating, the sample mass was recorded to understand the kinetics of their thermal decomposition. At 950 °C, the sample was maintained for 10 min, while the purge gas was changed to dry air. This step was carried out to combust the solid-char residue thus leaving behind only the ash contents. The mass-loss data from these tests allowed us to not only obtain the pyrolysis kinetics but also proximate analysis.

4.3 Lab-Scale Fixed Bed Reactor

Pyrolysis and CO_2-assisted gasification experiments were conducted using a lab-scale fixed-bed reactor system that was operated in semi-batch mode at different set temperatures of up to 1000 °C. The reactant gases flowed through the reactor continuously along with the product gases while for any given test, the sample feedstock was introduced as a batch of fixed mass. This reactor system was powered by two electric furnaces—Lindberg/Blue M Mini-Mite for preheating the incoming gases and Lindberg/Blue M 1200 °C Split-hinge tube furnace for sample heating at any defined temperature. The input gases included N_2 as the tracer gas, CO_2 as gasifying agent, and Ar to purge residual gases from the system. The flow rates of these gases were controlled separately using orifice flow meters. The evolved product gases were collected in sampling bottles (for short sample interval collection) or transported directly to a gas chromatograph for detailed analysis of the gases evolved. The feedstock sample holder was made of stainless-steel wire mesh, and this was inserted into the uniform heated zone of the reactor system at appropriate time via a quick-disconnect coupling at back end of the reactor. A schematic diagram of the

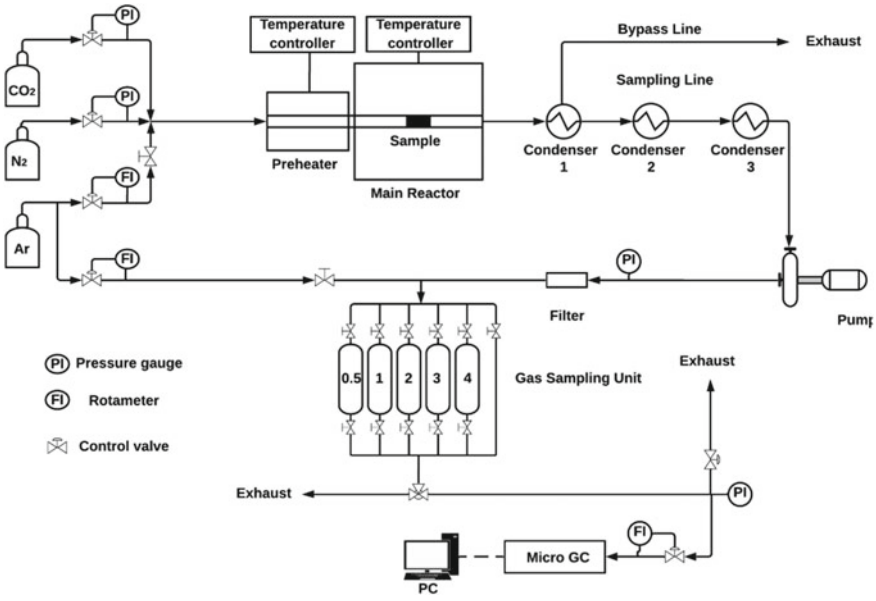

Fig. 2 Schematic of the experimental setup used for pyrolysis and gasification [15]

experimental setup details is provided in Fig. 2. The setup was equipped with ice-bath condenser and particulate filters to cool the product gases and remove moisture, tar and other particulate content in the product gases prior to their transport for gas analysis. Online product gas analysis was carried out using gas chromatography-thermal conductivity detector (GC-TCD) (Agilent Micro GC 3000A) which was calibrated for the quantification of mole fractions of H_2, CO, CO_2, CH_4, C_2H_4, C_2H_2, C_2H_6, O_2 and N_2 (using Restek refinery gas standard #1). The time required for each sample for gas analysis was almost 2.6 min. Additionally, the online gas sampling system was also equipped with gas sampling bottles in case of requirement of sampling times faster than 2.6 min. The electrical furnaces were monitored for their energy consumption (EML-2000, Canada) to estimate the energy requirements of each of the pyrolysis and gasification tests to obtain accurate values of overall energy efficiency beyond typically reported on energy recovery data. The char samples were characterized for their morphology using scanning electron microscopy (JSM-6510, Japan) at beam voltage of 20 kV after these samples were sputtered with Pt for better scanning characteristics. The char samples were also characterized for their surface area and pore volume using surface area and porosity analyzer (Tristar II 3020, USA).

Each test began by first allowing the input gases to go through the reactor system while the two furnaces reached the desired set point temperatures. The temperatures of interest were from 700 to 1000 °C. The input gases were chosen depending on the test conducted. For pyrolysis and co-pyrolysis tests, 2.1 sccm of N_2 flowed while avoiding entry of any other gas to maintain inert conditions during purging and analyzing the evolved gases. In the case of CO_2 gasification, a gas mixture of 75

vol.% CO_2 and 25 vol.% N_2 with a total flow rate of 2.1 sccm was used to allow for CO_2-assisted gasification. Here the vapor residence times were comparable to that in pyrolysis tests. Once the setpoint temperature was attained and the gas flow rates fixed, the sample holder containing 35 g of feedstock sample was inserted into the main reactor via quick-disconnect coupling. Tested feedstock samples included waste tire, pine bark and their mixtures at varying relative mass fractions of 1:3, 1:1 and 3:1 to not only analyze the influence of the mass ratio but also compare the results with the weighted results from separate processing of pure feedstocks to examine any possible interaction. While most of the product gases evolved from the main reactor were vented out, a fraction of it passed through the ice-bath condenser system that removed moisture and tar prior to analyzing the product gases. This dry and tar-free syngas were collected at 0.5, 1, 2, 3, 4 min from the start of the reaction using sampling bottles as such short sampling times of 1 min were not possible for online gas analysis using micro-GC and that our previous tests using different feedstocks had revealed that during this time, most of the syngas was released. From 5 min, this syngas was sent directly to the micro-GC for direct online gas analysis where the gas was collected at time intervals of 2.6 min and analyzed for the mole fractions of different gases against the calibrated gases.

$$M_i = \frac{X_i}{X_{N_2}} * V_{N_2} * \rho_i \tag{1}$$

Using the mole fraction of each gas species with respect to mole fraction of N_2, the gas flow rate of each of the gas species was calculated as the flow rate of N_2 was constant and it did not change during the reaction. From the known flow rate of N_2, it can be used as internal calibration reference to measure the flow rate of each of the gas species using the Eq. (1). In this equation, X_i is the measured mole fraction of species '*i*' at given time, V_{N_2} is the volumetric flow rate of N_2 at the reactor inlet, ρ_i is the standard density of species '*i*' and M_i is the mass flow rate of species '*i*' at given time. This method of obtaining gas flow rates assumes ideal gas behavior of the species, the inertness of N_2 toward these reactions, and that the syngas sample composition is representative of the composition of the evolved syngas prior to venting. Additionally, since each gas sample was collected over span of 10 s, this data represented an averaged value over that timespan at each time duration. This was carried out until the syngas at the GC was negligible. Ar was used to flush the reactor system and sampling lines of residual gases between each test. After this, the gas samples from sampling bottles were analyzed individually using micro-GC while Ar flushing was carried between the analyses for each of these bottles. The operating conditions of this experimental setup are summarized in Table 7.

Table 7 Summary of the operating reactor conditions for pyrolysis and gasification tests [15]

Pyrolysis	
Reactor temperature	673, 773, 873, 973, 1073, and 1173 K
Operating pressure	Atmospheric
Tracer gas and inert medium	2.1 sccm of N_2 (at standard 294 K and 1 atm.)
Sample	35 g of waste tire 2 × 2 cm pieces (60% tread and 40% sidewall)
Apparent vapor residence time	~21 s
Isothermal reaction time	2.5 h
Gasification	
Reactor temperature	973, 1073, 1173, and 1273 K
Operating pressure	Atmospheric
Tracer gas and inert medium	2.1 sccm of 75% vol. CO_2 and 25% vol. N_2 gas mixture (at standard 293 K and 1 atm.)
Sample	35 g of waste tire 2 × 2 cm pieces (60% tread and 40% sidewall)
Apparent vapor residence time	~21 s
Isothermal reaction time	53 min

5 Results and Discussion

5.1 Thermogravimetric Analysis

5.1.1 Waste Tire Decomposition

This analysis was carried out for gaining insights into the pyrolytic kinetics and its associated mass-loss behavior during the thermal decomposition of waste tire. This is essential as it provides us with the characteristic temperatures of decomposition and possibly also the compositional details of the rubbers used in the examined waste tire sample. With inert operation of TGA tests, one could quantify the volatile content sourced from the rubbers, accelerators and other additives present in the tire. The combustion step using air at high temperature was carried out to quantify the inorganic content and the fixed carbon content (mostly carbon black) in the case of waste tire. TGA tests in CO_2 environment were avoided since the decomposition here is slow and at their characteristic temperatures (due to low heating rate) which were significantly low for CO_2 to be active. Additionally, to normalize the mass-loss data obtained from TGA into non-dimensional format, conversion (α) was obtained, and the results are reported using this data and its derivative with respective to instantaneous temperature (DTG $= \mathrm{d}\alpha/\mathrm{d}T$). Normalization was carried out according to Eq. (2), where $M(T)$ is the mass of the remaining sample in the TGA at temperature T, T_o is the initial temperature (100 °C) and T_f is the final temperature (950 °C).

$$\alpha(T) = \frac{M(T_o) - M(T)}{M(T_o) - M(T_f)} \tag{2}$$

This conversion data for thermal decomposition of waste tire is presented in Fig. 3 along with DTG (derivative with respect to temperature). These results show similarity compared to those reported in the literature. The DTG data is useful to represent the behavior of waste tire decomposition and reveals the volatile evolution to be a combination of three stages (i.e., showing three peaks) at temperatures of 450–600 K, 600–680 K, and 680–800 K. Each of these regions could be a combination of decomposition patterns from different constituents, such as decomposition of unstable additives such as extender oils and other low-boiling point additives that contribute to the first stage of decomposition while the second stage could be from natural rubber (NR) decomposition and initiation of decomposition of polybutadiene rubber (BR), and styrene-butadiene rubber (SBR). The third stage could be significantly from the decomposition of BR and SBR based on the straight elastomer and is based on the TGA studies reported in the literature [41]. Most of the literature on such analysis of tires has reported the latter two stages corresponding to elastomers decomposition and in some cases, the second stage contributed more to the mass-loss than the third due to different proportions of the rubber mix. The high mass-loss from the third peak revealed that the specific waste tire examined here contained significantly high BR and SBR proportions compared to NR and that the ratio of BR to SBR could be predicted from the position and contribution of the third peak based on the literature reported on varying ratios.

$$\begin{aligned} \mathrm{DTG}_{\text{waste tire}} = {} & w_{\mathrm{NR}} * \mathrm{DTG}_{\mathrm{NR}} + w_{\mathrm{BR}} * \mathrm{DTG}_{\mathrm{BR}} \\ & + w_{\mathrm{SBR}} * \mathrm{DTG}_{\mathrm{SBR}} \end{aligned} \tag{3}$$

To quantify the relative composition of individual rubbers in the waste tire examined, we employed a three-component curve-fit to the DTG data based on the straight

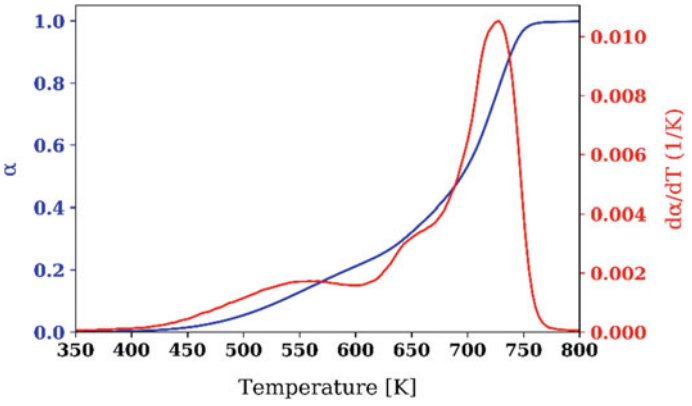

Fig. 3 Extent of mass-loss (α) and its derivative with temperature during waste tire pyrolysis [15]

Table 8 Estimated composition of elastomers in the tested waste tire [15]

Polymers	Composition (wt.%)
Natural rubber (NR)	5
Butadiene rubber (BR)	40
Styrene–butadiene rubber (BR)	55

elastomer DTG data from the literature, neglecting the presence of any interaction's contribution to the mass distribution and additives contribution to the mass-loss in the latter two stages. Equation (3) revealed that the equation used to represent such a model was favorable, where w_i represent the mass fraction of the respective elastomer in the waste tire, and the DTG_{NR}, DTG_{BR} and DTG_{SBR} were DTG of the respective straight-chain elastomers obtained from the literature. The $DTG_{waste\ tire}$ obtained from our data and the fit obtained had a coefficient of correlation of $R^2 = 0.996$. The estimated compositional results from this analysis are given in Table 8 that reveals significant presence of BR and SBR.

5.1.2 Decomposition of Waste Tire-Pine Bark Blend

Investigations involving TGA on blends of waste tire with other feedstocks are essential to understand the presence of any interaction and establish the feasibility of a feed-flexible gasifier where waste tires can be converted in the presence of any other feedstocks for sustainable operation and avoid over dependence on any individual feedstock. For this, blends of waste tire and pine bark were mixed in defined fraction and ground into similar size powder form. The relative fractions of each in the blends were 1:1, 1:3 and 3:1. These samples will be represented by *WxPy* where *x* represents waste tire mass fraction and y represents pine bark mass fraction; for example, W1P3 represents a sample with 25 wt.% waste tire and 75 wt.% pine bark. The results from these blends will be compared with the calculated weighted results from the individual components. Figure 4 reveals the conversion and DTG behavior

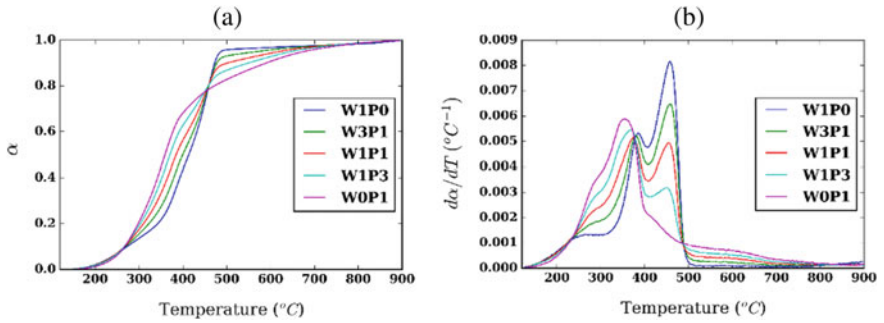

Fig. 4 Effect of waste tire-pine bark mixture ratio on **a** the extent of mass-loss, α, and **b** its derivative [18]

of the blends in comparison with pure components—waste tire (W1P0) and pine bark (W0P1). Pine bark also exhibited the presence of multiple peaks corresponding to the decomposition of lignocellulosic components such as hemicellulose, cellulose and lignin, respectively, with increase in temperature. Note that lignin partially contributed to all the stages of decomposition. Pine bark decomposition started early from 220 °C while waste tire pyrolysis was concentrated between 250 and 550 °C. Comparison of blended DTG with weighted results (not shown here), i.e., comparing DTG_{WxPy} with $(x*DTG_{\text{waste tire}} + y*DTG_{\text{pine bark}})/(x + y)$, revealed the lack of any difference in behavior. Although this reveals the lack of any synergistic interaction between waste tire and pine bark, it is important to note the lack of any inhibitive behavior either. This means that the decomposition of either components was possibly occurring independent of each other. This also means that conversion of waste tire in the presence of biomass feedstocks such as pine bark can be carried out in the same reactor without the loss of any efficiency and easily predict the decomposition behavior without any issues of interaction. Although any interaction seems to be missing according to the DTG behavior, further lab-scale studies were also carried out via pyrolysis and CO_2 gasification to confirm such behavior and observe for any high-temperature, heating rate effects and volatile–volatile interaction behaviors that cannot be observed from TGA results. Such a behavior on the lack of interaction from TGA results but presence of significant synergistic interaction during lab-scale high temperature gasification and pyrolysis was observed in various biomass–plastic mixtures such as pinewood–polyethylene. The lab-scale studies described here in the later sections revealed the observation of such a synergistic behavior.

5.2 Lab-Scale Pyrolysis and Gasification

5.2.1 Product Gas and Char Yield

Waste Tires

Online gas chromatography analysis was used to analyze and quantify dry, tar-free and particulate-free product gases for H_2, CO, CO_2, CH_4, C_2H_4, C_2H_6 and C_2H_2 as they represent the major compounds evolved from pyrolysis and gasification of tires. In this chapter, we refer to the combination of H_2, CO, CH_4, C_2H_4, C_2H_2 and C_2H_6 as syngas since these components are important due to their calorific value, while the combination of this syngas with CO_2 will be referred to as product gas since one can consider CO_2 as a by-product. From the mass flow rates obtained with time for different temperatures, cumulative yield of these components was calculated over a 50-min time duration for both pyrolysis and gasification to understand the influence of temperature and gasifying agent on the syngas evolution and thus the carbon conversion. Char yields were also measured at the end of reaction for these conditions to gain insights into the tendency of charring and the loss of yield by forming char as by-product.

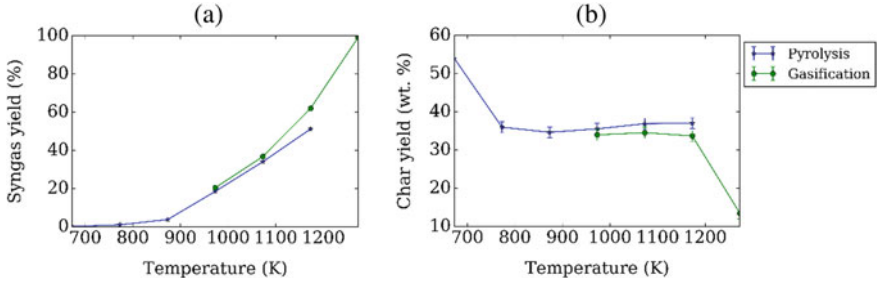

Fig. 5 Effect of temperature on **a** syngas and **b** char yield during pyrolysis and CO_2-assisted gasification of waste tires [15]

Figure 5 reveals the variation of syngas and char yield (as wt. % of waste tire mass after 2.5 h) with temperature and gasifying agent. At lower temperatures of 700–800 K, insignificant amounts of syngas evolved due to the inability of conversion of the volatiles evolved from waste tire to further crack or interact with CO_2 to form any of the evolved syngas components examined. But, at these temperatures char yield was more than 50% that decreased to ~38% as the temperature was increased to beyond the maximum temperature of complete conversion (~770 K) as seen from the DTG results presented in Fig. 3. From 800 K, syngas yield increased strongly with temperature because at high operational temperatures of the lab-scale reactor, the sample experienced high heating rates immediately after placing it in the reactor, leading to increased volatiles evolution. These volatiles undergo secondary reactions such as thermal cracking, and CO_2-reforming in the gas phase leading to the formation of syngas components. These gas-phase reactions leading to the formation of H_2, CO and light hydrocarbons are endothermic and thus with increase in temperature, the syngas yield is enhanced. In the case of gasification, temperatures above 973 K are required for CO_2 to actively react with the intermediates from the decomposing waste tire. Syngas yield as high as 50% from pyrolysis and 100% from gasification was obtained from waste tire conversion. The literature also reported high gaseous yields and were dependent on the reactor used to obtain high temperatures and heating rates, high vapor residence times and slow quenching that provided the necessary conditions for enhanced secondary reactions of cracking and reforming in the gas phase. Comparing the yields from pyrolysis and gasification, increase in temperature increased the differences in the gas yield as the char reforming reactions also contributed leading to improved CO yields.

In the case of char yield, beyond the temperature of complete devolatilization from TGA results (770 K), the char yields did not change significantly with temperature during pyrolysis as the char obtained was stable, similar to the char residue from TGA results. But in the case of gasification, beyond 1173 K, the char yield decreased significantly by about 50% due to Boudouard reaction of the char with CO_2 which was only active at high temperatures beyond 1100 K based on our previous studies on CO_2-assisted gasification of various other kinds of feedstocks.

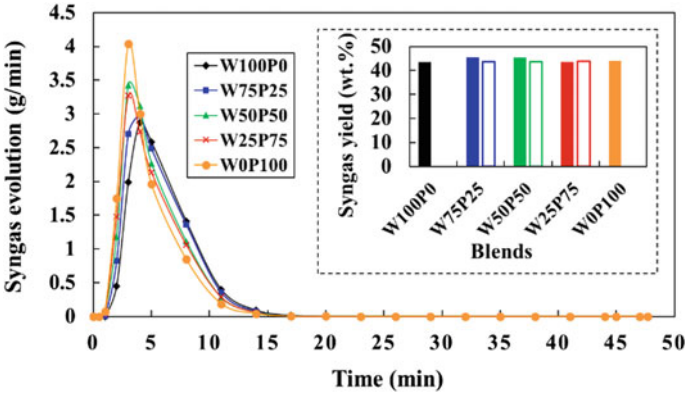

Fig. 6 Effect of waste tire-pine bark blend ratio on the evolution behavior and yield of syngas during co-pyrolysis at 900 °C (solid bars: experimental; hollow bars: weighted yields) [4]

Waste Tires with Pine Bark

Investigations into co-pyrolysis and co-gasification of waste tires with pine bark at 900 °C were conducted using lab-scale reactor system to examine any possible interaction. Figure 6 shows the influence of feedstock mixture fraction on the syngas yield during co-pyrolysis in comparison with estimated yields calculated by weighted aggregate of the individual feedstocks processed separately. The syngas yields revealed no significant interaction between waste tire and pine bark pyrolysis when processed together as the blend co-pyrolysis yields were similar to the weighted yields. At the examined temperature, the syngas yield was found to be ~40 wt.% for all the blend samples and pure samples. This was probably due to the high thermal stability of fixed carbon in waste tire leading to its low reactivity toward pine bark pyrolysis. Variation of char yield after 48 min with blend ratio during co-pyrolysis was also measured, and the results are shown in Fig. 7. While no significant interaction was observable, as the differences between the yields from co-pyrolysis and the weighted yields were negligible, the yield decreased with increase in pine bark content due to relatively high charring tendency from waste tire from its fixed carbon compared to pine bark.

Co-gasification was carried out at both 800 and 900 °C under similar conditions as in our other gasification studies but at different blend ratios. Figure 8 reports the influence of feedstock mixture on the syngas yield at these temperatures. The results obtained showed a decrease in syngas yield from co-gasification at 800 °C compared to separate feedstock gasification, but no such inhibition was observed at 900 °C. Further investigation into the composition of the syngas can provide us with information about any such interaction.

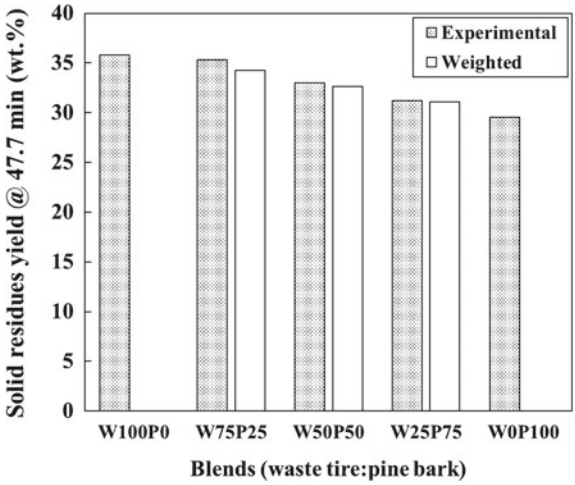

Fig. 7 Effect of feedstock blend ratio on the char yield from co-pyrolysis of waste tire and pine bark at 900 °C [4]

5.2.2 Syngas Components' Evolution and Yield

Waste Tires

From online product gas analysis capabilities using our lab-scale reactor system, we were able to obtain the temporal evolutionary behavior of flow rates of syngas and its components. Figure 9 reveals the impact of temperature on the evolutionary behavior of syngas during pyrolysis and gasification from the waste tire sample. The flow rate curves showed peak, and with increase in temperature, the peak value increased, but its position shifted toward earlier (shorter) times. This is because increase in temperature not only drives the equilibrium toward syngas product due to the global endothermicity of both pyrolysis and CO_2-assisted gasification, but also improves the kinetics of these reactions. This behavior was observed in the evolution of all the major components of syngas; see Fig. 10. Hydrogen (H_2) and CH_4 were the dominant components impacted by the temperature change during pyrolysis while CO and H_2 during CO_2-assisted gasification. While the evolution of syngas flowrate completed in 25 min during pyrolysis, it decreased to a constant nonzero value during CO_2-assisted gasification and then stayed at that flow rate for extended periods of time; see Fig. 10. CO evolution showed similar behavior that extended for a long period of time during CO_2-assisted gasification. During this process, the contribution of CO to syngas yield was very high. This was due to low reactivity of tire-char residual with CO_2 after 25 min, possibly due to high crystallinity, low imperfections and O, H content, and low surface area compared to other carbonaceous materials such as biomass. Long gasification times were reported to be required even in the case of steam gasification despite relatively higher reactivity of tire char with steam compared to CO_2.

Figure 11 reveals the cumulative yields of the individual syngas components and their variation with temperature during pyrolysis and CO_2-assisted gasification, while

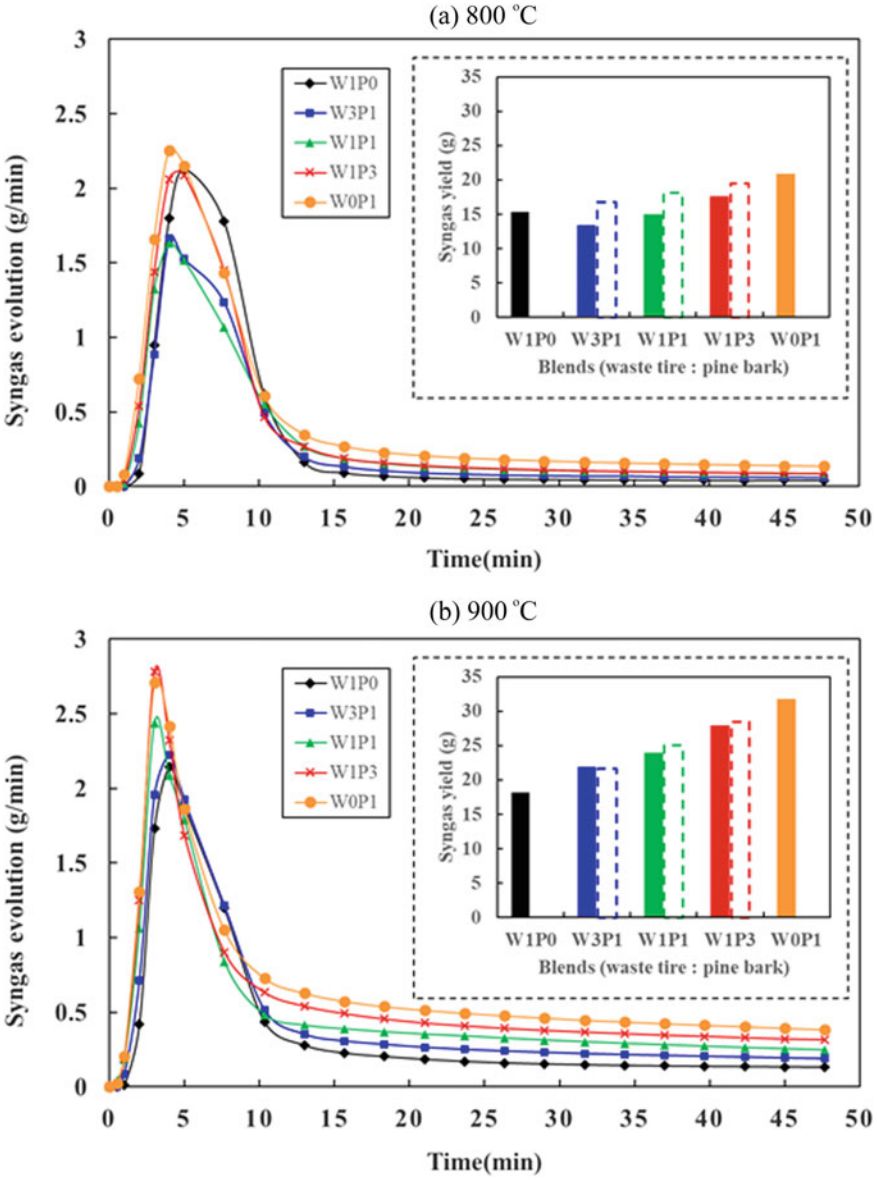

Fig. 8 Effect of feedstock blend ratio on the syngas yield from co-gasification of waste tire and pine bark at **a** 800 °C and **b** 900 °C [18]

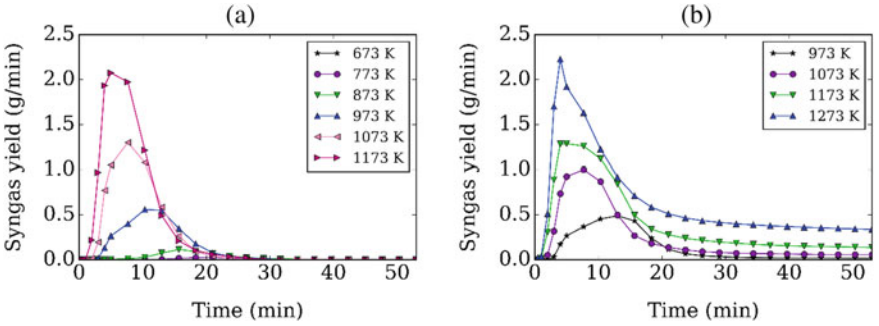

Fig. 9 Effect of temperature on the evolution of syngas from waste tires under **a** pyrolysis and **b** gasification [15]

Fig. 12 shows their mole fraction in cumulative product gas yield (including CO_2). In pyrolysis, increase in temperature increased the yields of H_2, CO, CH_4 and C_2 hydrocarbons. During pyrolysis, decarboxylation and decarbonylation occur of the oxygenates in the waste tire such as extender oils, secondary reactions with char, along with decarboxylation of inorganic content such as $CaCO_3$, $CaSiO_4$ and other metal carbonates. Low molecular mass hydrocarbons (CH_4, and C_2) were generated by gas-phase cracking of the volatiles released from the decomposition of BR and SBR polymers in addition to H_2. Hydrogen is also released from aromatization and cyclization of the volatiles in the gas phase, while these reactions are significantly enhanced with temperature. Comparing the H atomic content in waste tire (from ultimate analysis shown in Table 6) with the yields of H_2 and CH_4 revealed that significant portion of H content in the solid sample got converted to syngas.

Figure 12 reveals that while the net CO_2 yield enhanced with temperature, its mole fraction in product gas decreased. At low-temperature pyrolysis, while decarboxylation reaction is favored to release CO_2, insignificant conversion of heavy hydrocarbon intermediate volatiles into syngas components resulted in high CO_2 mole fraction. As the temperature increased, other components enhanced due to the contribution of enhanced secondary gas-phase reactions at a higher rate leading to the observed net reduction in CO_2 mole fraction. This is also because of enhanced equilibrium drive toward higher CO content at high temperature compared to CO_2. This enhanced thermal cracking of heavy intermediates from rubber components can be seen from enhanced CH_4 mole fraction in product gas; see Fig. 12. However, in the case of CO_2-assisted gasification, this increase in mole fractions of CH_4 and C_2 with temperature is met with opposing reactions such as dry hydrocarbon reforming to form H_2 and CO which results a decrease in these hydrocarbon mole fractions beyond 1173 K. Equations (4)–(11) represent the major reactions during pyrolysis and gasification of waste tires and biomass. Improved rate of increase in CO yield due to Boudouard reaction also contributed to the lowered hydrocarbon yields at high temperature; see Eq. (5).

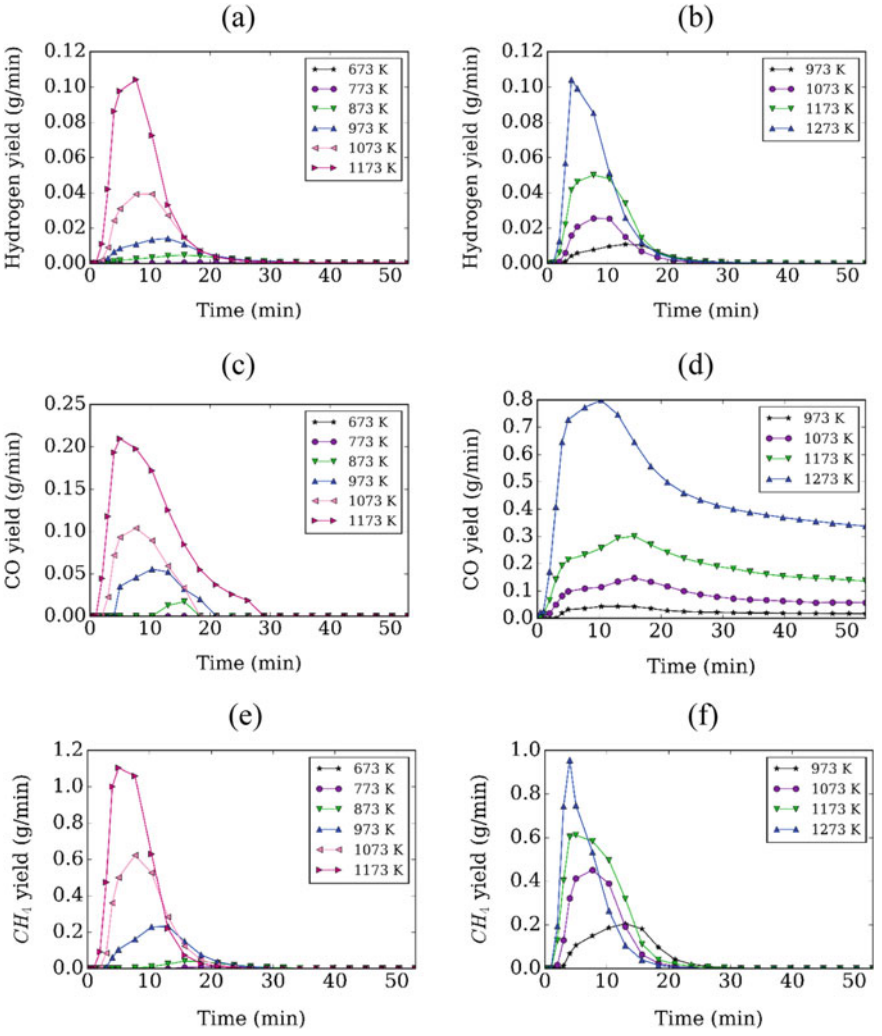

Fig. 10 Effect of temperature on the evolution of H_2, **a**, **b**, CO, **c**, **d** and CH_4, **e**, **f** during pyrolysis (left) and CO_2-assisted gasification (right) of waste tires [15]

$$\begin{aligned}&\text{Waste tire} + \text{pine bark} + CO_2\\ &\quad\rightarrow\ H_2 + CO + CO_2 + CH_4 + C_mH_n\\ &(C_2H_2 + C_2H_4 + C_2H_6 + C_3H_8 + \ldots)\\ &+ H_2O + \text{char} + \text{tar}\ \Delta H > 0\end{aligned} \tag{4}$$

$$C + CO_2 \rightleftharpoons 2CO \quad \Delta H = +172\,\text{kJ/mol} \tag{5}$$

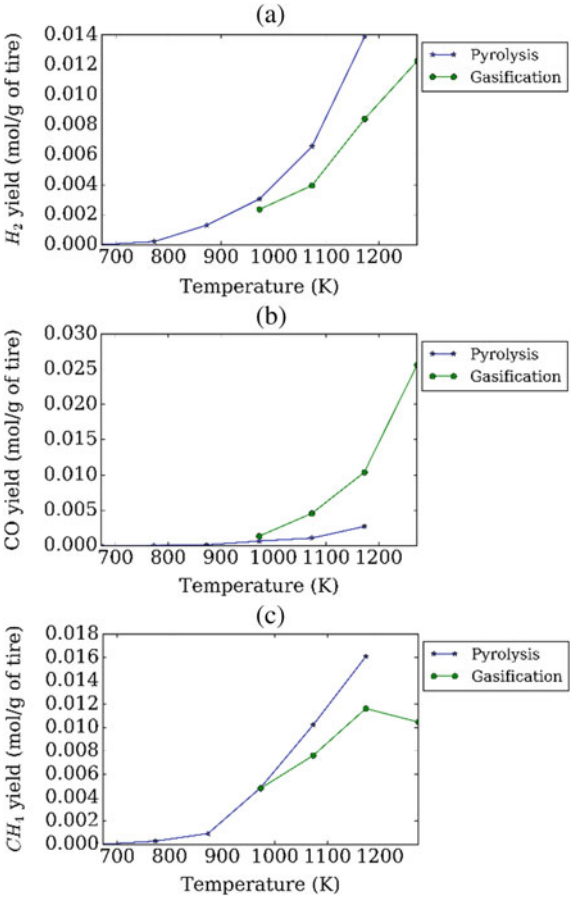

Fig. 11 Effect of temperature on the cumulative yields of **a** H_2, **b** CO and **c** CH_4 from pyrolysis and CO_2-assisted gasification of waste tires [15]

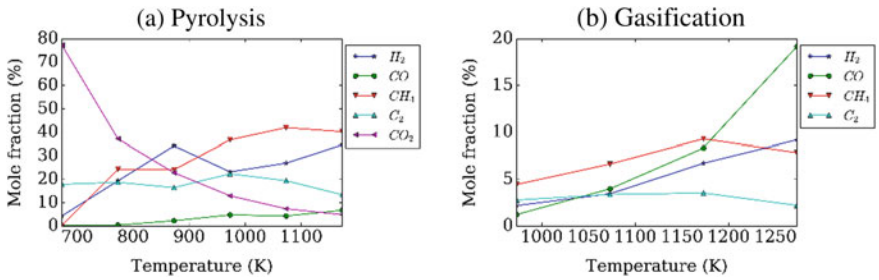

Fig. 12 Effect of temperature on the mole fractions of individual species from cumulative syngas yield from **a** pyrolysis and **b** CO_2-assisted gasification of waste tires [15]

$$C + 2H_2 \rightarrow CH_4 \quad \Delta H = -75\,\text{kJ/mol} \tag{6}$$

$$C + H_2O \rightarrow CO + H_2 \quad \Delta H = +131\,\text{kJ/mol} \tag{7}$$

$$CO + 3H_2 \rightleftharpoons CH_4 + H_2O \quad \Delta H = -206\,\text{kJ/mol} \tag{8}$$

$$CO_2 + H_2 \rightleftharpoons CO + H_2O \quad \Delta H = 41\,\text{kJ/mol} \tag{9}$$

$$\text{Tar}\left(C_xH_y\right) + xCO_2 \rightarrow 2xCO + (y/2)H_2\Delta H = 0.9\,\text{to}\,0.3\,\text{MJ/mol} \tag{10}$$

$$\text{Tar} \rightarrow CH_4 + H_2 + H_2O + C_mH_n \quad \Delta H > 0 \tag{11}$$

Equations (5), (7), (9) and (10) contribute to provide significant enhancement of CO yield with increase in temperature, and the rate of increase was higher at high temperature. At temperatures beyond 1073 K, CO yield increased with temperature by 1.5 times/100 K to provide yields as high as 25.6 mmol/g which accounted for 0.72 g per gram of waste tire feedstock. Below this temperature, the yield of all the syngas components from CO_2-assisted gasification was almost the same as that from pyrolysis due to low activity of CO_2 at these temperatures. TGA results and literature also reveal this to be the case while this also supports CO_2-assisted gasification to be an extension of pyrolysis to include CO_2 reforming of the evolving volatiles and char into CO and H_2; see Figs. 5 and 10 that reveal lowered hydrocarbon and char yields with increase in CO yield compared to pyrolysis at high temperatures.

Waste Tires with Pine Bark

To investigate further into any possible synergistic or inhibitive interaction between waste tire and pine bark during their co-processing via pyrolysis and CO_2-assisted gasification, we examined the evolution of syngas components and yield and compared the results with the weighted data calculated from separate conversion of the feedstock. The weighted yields were calculated with the initial mass fraction of the feedstock components to be their respective weights in the aggregate.

Figure 13 reveals the influence of feedstock mass fraction on the variation of major syngas components' mass flow rate with time along with their cumulative yield compared with weighted yields during co-pyrolysis. The results reveal the yields from blended feedstock to be almost same as the weighted yields from mono-conversion. This means that in pyrolysis to obtain gaseous yields, waste tire and pine bark feedstock show no interaction with each other and the behavior of the reaction products was a superimposition of their behavior when pyrolyzed separately. This

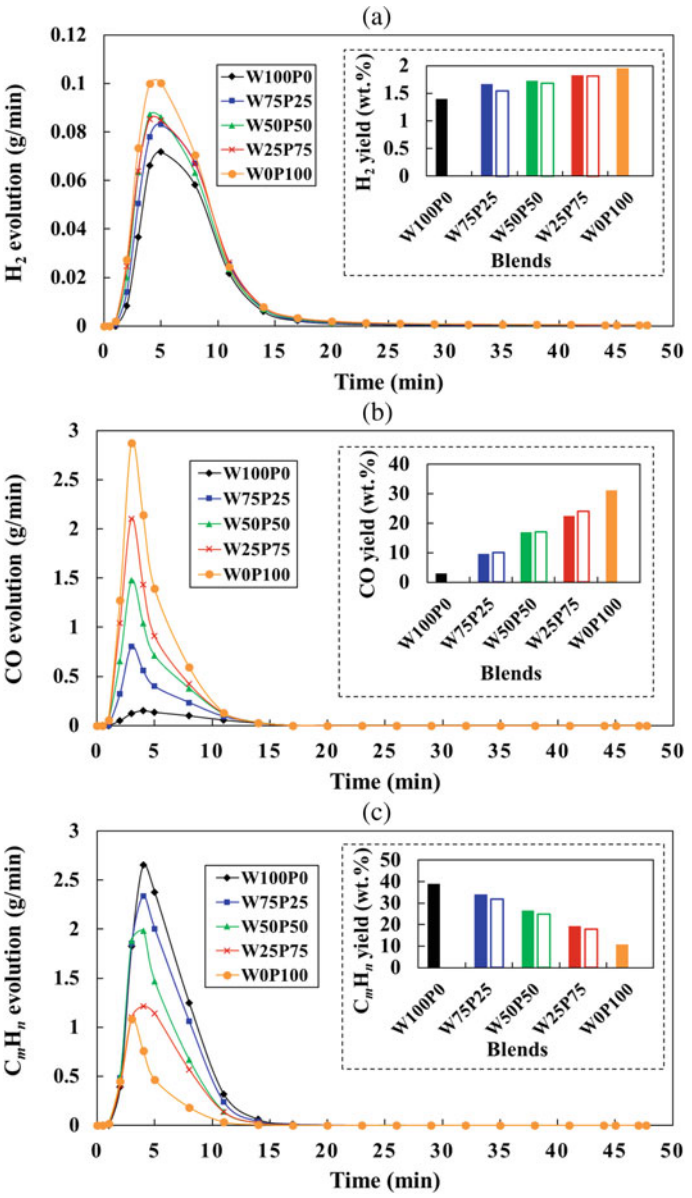

Fig. 13 Effect of feedstock blend fraction on the evolution and yield of **a** H_2, **b** CO and **c** C_nH_m from co-pyrolysis of waste tire and pine bark [4]

simplifies the modeling and design of feed-flexible reactors as it alleviates the need for any further studies into nonlinear behavior. Additionally, this also provides the design option to modify the syngas composition and their respective component yield by modifying the mixture composition of the feedstock. While the syngas yield did not change significantly with the feedstock in the case of co-pyrolysis, hydrocarbon yield was favored with high waste tire content, while CO yield was favored with high pine bark content, due to oxygenates present in the biomass. H_2 yield also increased with increase in pine bark content but to a lesser extent compared to other species. As the net syngas yield was almost the same for all the feedstock mass fractions, it suggests that the decreased mass of C_nH_m with increase in pine bark was appropriately compensated by the increase in CO mass yield. The variation in CO yield varied from less than 5 wt.% from pure waste tire pyrolysis to almost 30 wt.% from pure pine bark, while C_nH_m yield varied between 40 wt.% from pure waste tire to ~10 wt.% from pure pine bark.

Similar data showing the evolution of syngas components and their yield is reported in Fig. 14 for both 800 and 900 °C that not only provide information about the variability on the evolutionary behavior with feedstock variation, but also provide insights into possible interaction that could lead to non-additive yields. Increase in temperature led to significant increase in the peak H_2 mass flow rate from ~0.035 g/min to as much as ~0.075 g/min due to enhanced cracking and CO_2-reforming. Increase in pine bark content also increased the H_2 flow rate and yield due to the higher reactivity of the biomass to react with CO_2 to form H_2 and CO. At 800 °C, some variation between the H_2 yields from the blends and the weighted results was found. However, at 900 °C, these differences disappeared to finally provide blended yields same as the weighted yields. CO flow rate and yield also increased with increase in pine bark content not only due to its higher reactivity compared to waste tire but also due to inherently higher oxygenate content in the biomass. The CO yield also increased with temperature by almost twice from 800 to 900 °C due to enhancement of CO from pyrolysis along with char gasification and CO_2-reforming. The behavior of CO flow rate with time showed not only a peak but also a steady CO yield from ~10-min time due to Boudouard reaction involving char-CO_2 gasification to provide enhanced CO yields. Such a constant flow rate was due to slow reaction rate of the char with CO_2, possibly due to low porosity. Synergistic reduction of C_nH_m was also found at 800 °C, which also led to lower syngas yield, as seen from Figs. 8 and 14. But this was not observed at 900 °C, possibly due to higher influence of gas-phase reactions with CO_2 leading to similar yields as the weighted yields.

From these results, we can see that at operational temperatures of 900 °C required for CO_2-assisted gasification, the syngas component yields from co-gasification were superimposed sum of the yields from individual components to prove the compatibility of waste tire with biomass gasifiers. So, subject to the net product output required, the feedstock can be modified to include waste tires without the loss of conversion efficiency.

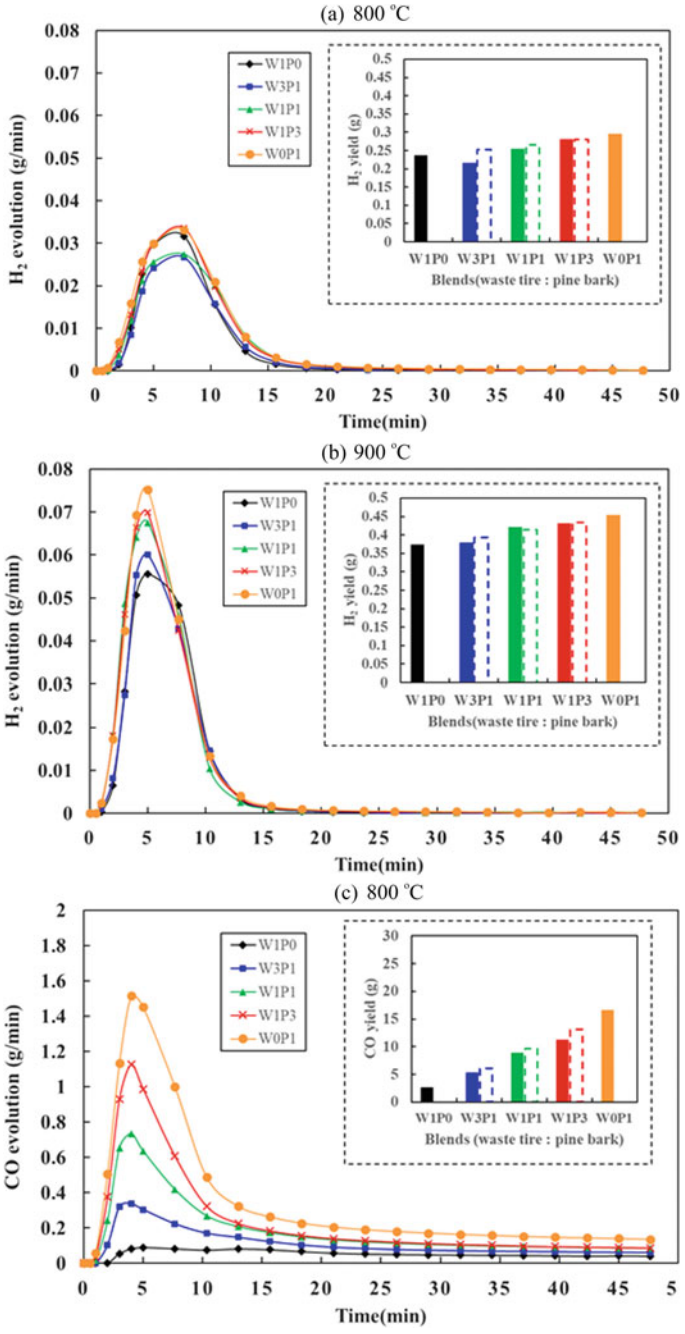

Fig. 14 Effect of temperature and feedstock blend fraction on the evolution and yield of **a**, **b** H_2, **c**, **d** CO and **e**, **f** C_nH_m from co-gasification of waste tire and pine bark at 800 °C and 900 °C, respectively [18]

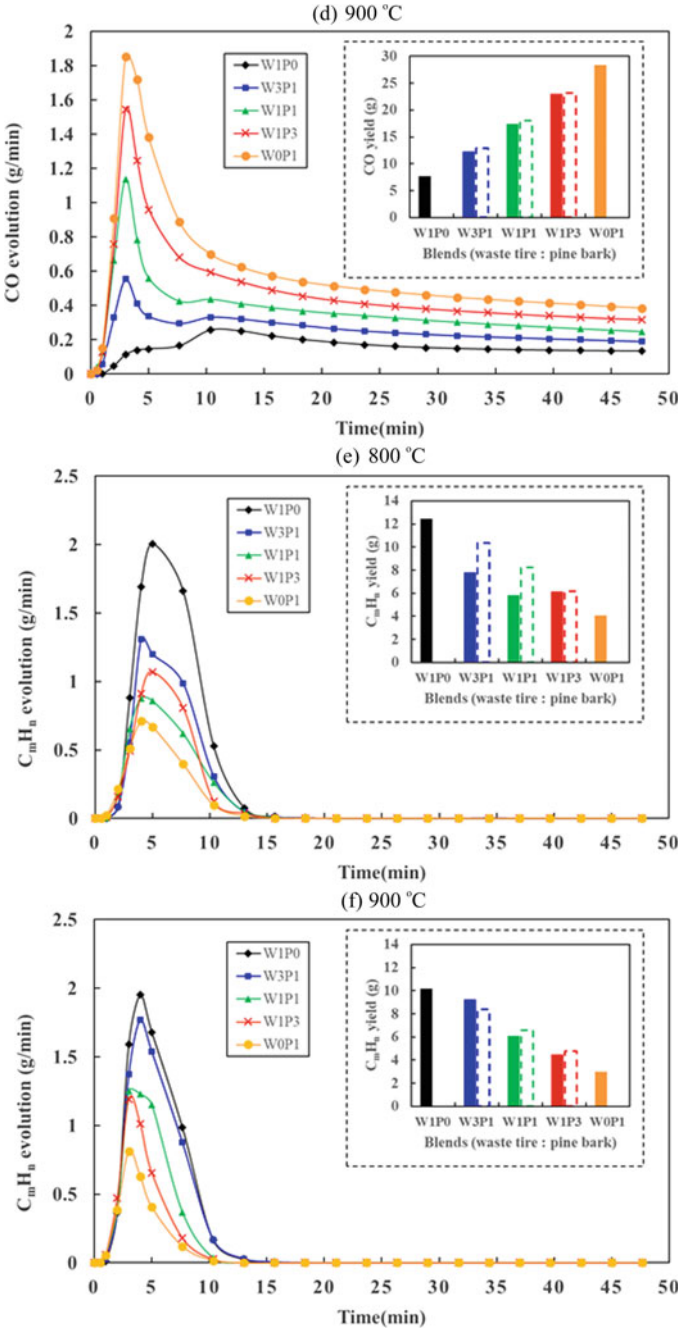

Fig. 14 (continued)

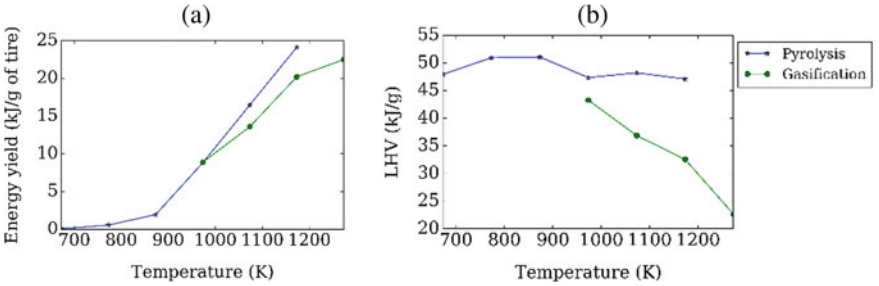

Fig. 15 Effect of temperature on **a** energy yield and **b** LHV of the syngas yield from pyrolysis and CO_2-assisted gasification of waste tire [15]

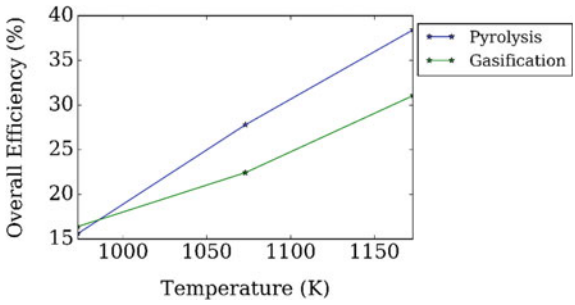

Fig. 16 Effect of temperature on the overall energy efficiency of pyrolysis and CO_2-assisted gasification of waste tire [15]

5.2.3 Syngas Energy Recovery and Overall Energy Efficiency

Waste Tires

The energy yield from pyrolysis and gasification in the form of calorific content of syngas was obtained by aggregating the yield of individual syngas components' yield multiplied with their respective lower heating value (LHV). Similarly, LHV of the CO_2-free syngas was also obtained by dividing the respective energy yield with the syngas yield to provide a perspective of the quality of flammable gases that can be obtained. From this energy yield, the overall energy efficiency was also calculated using the Eq. (12) which also considers the electrical energy consumed by the furnaces.

$$\text{Overall energy efficiency} = \frac{m_{\text{syngas}} * \text{LHV}_{\text{syngas}}}{\text{Energy}_{\text{input}} + m_{\text{feedstock}} * \text{LHV}_{\text{feedstock}}} \tag{12}$$

Figure 15 reveals the energy yield and LHV of the syngas, while Fig. 16 reveals the overall energy efficiency of both pyrolysis and CO_2-assisted gasification of waste tire. The energy yield increased with increase in temperature for both gasification and

pyrolysis although higher content of hydrocarbons in the syngas from pyrolysis led to higher energy yield from pyrolysis compared to gasification, which was dominated by CO yield due to higher LHV of hydrocarbons compared to CO. So, the energy yield and efficiency reported here are from the perspective of utilizing the products for energy recovery purposes. Pyrolysis yielded overall energy efficiency of almost 38%, while gasification yielded 30% to support the feasibility of waste tire conversion for energy recovery. Although this may seem relatively low, it only accounts for syngas energy and significant portions of energy were also transformed into char residue that offers its own value.

Waste Tires with Pine Bark

To further understand the energy yield and overall energy efficiency, variations obtained from co-pyrolysis and co-gasification of waste tire with pine bark were also examined. Additionally, to obtain accurate representation of the overall energy recovery feasibility, heating value of char residue was also measured and the calorific content of this char was also incorporated into the overall energy efficiency as the product energy output to observe the capability of our lab-scale reactor experiments in establishing the feasibility of this process. Additionally, studies incorporating pine bark also revealed the pathways of modifying energy input and output for better design of conversion reactors.

Figure 17 reveals the overall energy efficiency variation with time along with inset cumulative results of efficiency at different times that included consideration on char energy from co-pyrolysis. The variation with time reveals the efficiency to reach maximum at 10 min while beyond that temperature resulted in a slow decrease in the efficiency. At 15 min, the efficiency reached as high as 45% while considering only syngas energy, and by 47.7 min the efficiency reached to 35%. Note that reactors need to be designed by considering both the extent of conversion and the process efficiency. So, these results will provide with the required understanding to design reactors for high yield and efficiency along with optimal syngas composition. Incorporation of the char energy into efficiency after 47.7 min led to almost constant efficiency of 48% for all the waste tire-pine bark blends examined. This makes the overall process to be feasible and sustainable. Comparison of the energy efficiency from the blends with the weighted results, we can also see a slight non-additive synergistic enhancement in the efficiency when the feedstocks used were blends compared to separate pyrolysis. Such synergistic enhancement could form cumulative enhancement of all the syngas yields to a lesser extent contributing to an overall significance.

From these results, we can see that significant portions of the feedstock were converted into char leading to the limitations of efficiency. While the efficiency is acceptable, the char needs to be either converted for energy purposes or some other utility for better economic output from waste tire conversion. A combination of syngas production with extraction of char including carbon black for utilization in material applications is necessary for sustainable operation of this pathway. Figure 18 shows surface area of the char produced from co-pyrolysis of waste tire and pine bark.

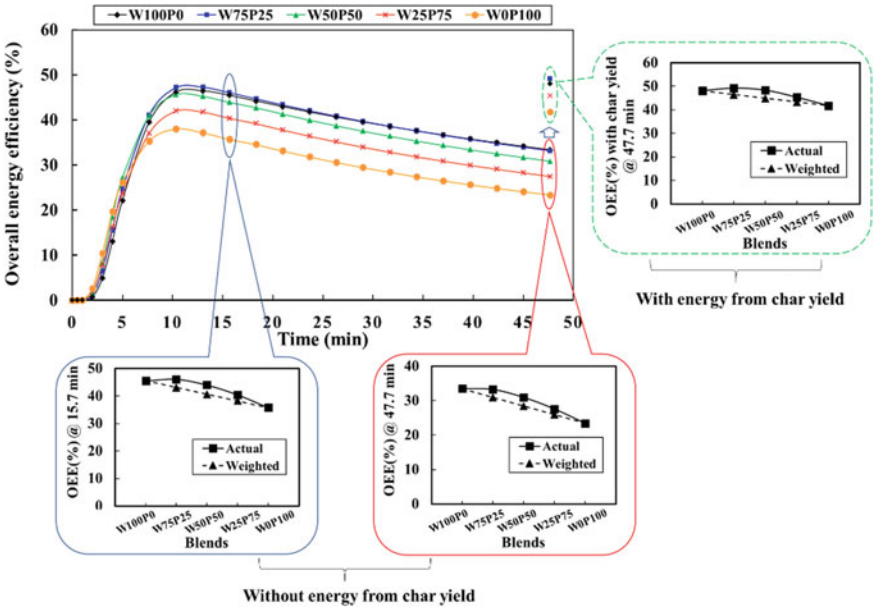

Fig. 17 Effect of feedstock blend fraction on the overall energy efficiency (OEE) from co-pyrolysis of waste tire and pine bark [4]

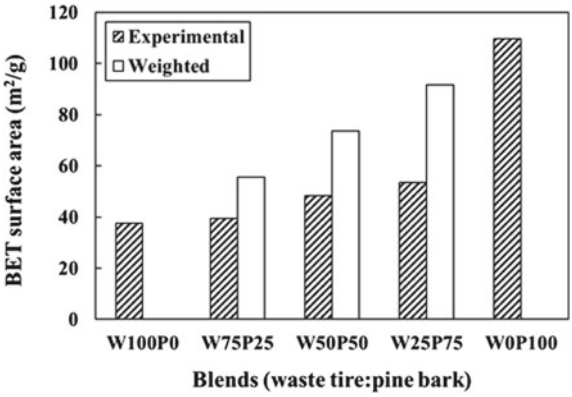

Fig. 18 Effect of feedstock blend fraction on the surface area of char residue from co-pyrolysis of waste tire and pine bark [4]

The results show relatively low-surface area from waste tire compared to pine bark, and their co-pyrolysis led to inhibitive lowered char surface area compared to separate pyrolysis. Figure 19 shows the difference in the morphology of chars from waste char and pine bark and their variation with co-pyrolysis. Further studies are essential to explore future direction toward the applicability of these chars for high-value purposes, such as carbon catalysts, activated carbon and other valuable carbon solid products to make thermochemical conversion of waste tires economically attractive.

(a) W:P=100:0 (1000×) waste tire

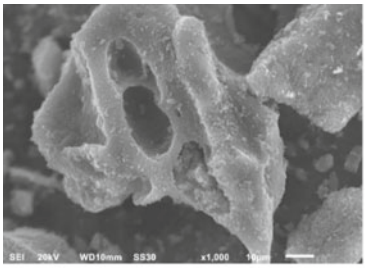

(b) W:P=0:100 (1000×) pine bark

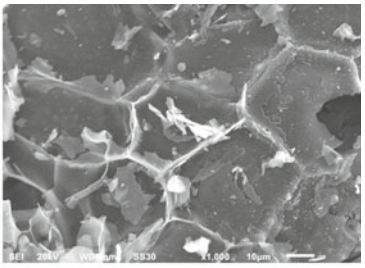

(c) Waste tire solid in W:P=75:25 (1000×)

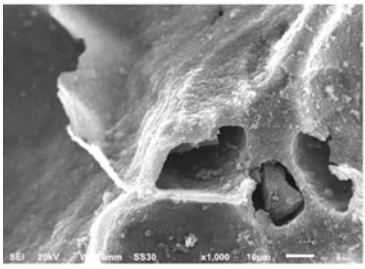

(d) Pine bark solid in W:P=75:25 (1000×)

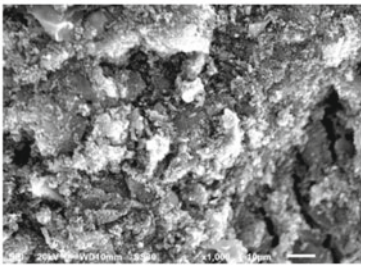

(e) Waste tire solid in W:P=50:50 (1000×)

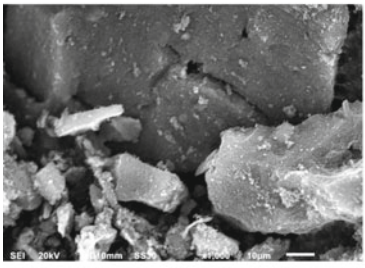

(f) Pine bark solid in W:P=50:50 (1000×)

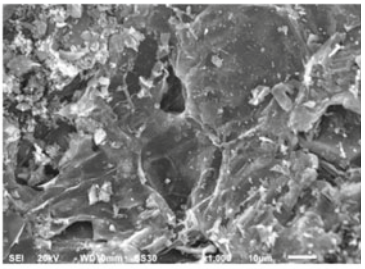

(g) Waste tire solid in W:P=25:75 (1000×)

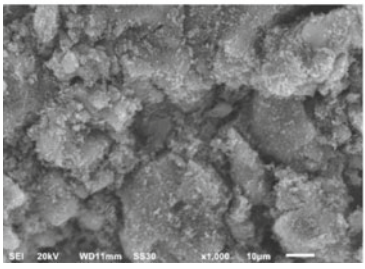

(h) Pine bark solid in W:P=25:75 (1000×)

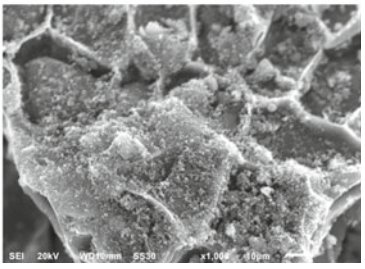

Fig. 19 Morphology of char residue from waste tire and pine bark during their co-pyrolysis at different blend ratios [4]

5.2.4 CO_2 Consumption During CO_2 Gasification

In addition to providing waste tire disposal and energy recovery, CO_2-assisted gasification also provided with positive utility to high-temperature CO_2 utilization and thus reduced net carbon emissions from this disposal process. In our studies, we characterized the capability of CO_2 gasification in CO_2 utilization by examining the net CO_2 consumption during the overall gasification process. This was carried out for both waste tire gasification and its co-gasification with different ratios of pine bark. Figures 20 and 21 reveal the influence of temperature and feedstock composition on the cumulative CO_2 consumption. Increase in temperature led to increase in CO_2 consumption with values as high as 0.7 g of CO_2 consumed per each gram of waste tire at 1000 °C. This consumption rises from the Boudouard reaction and gas-phase CO_2 reforming reactions which enhanced with temperature. Comparison revealed CO_2 consumption during pine bark conversion was higher than waste tire conversion.

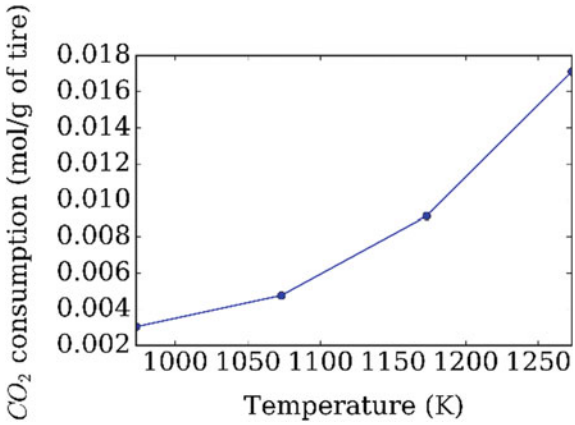

Fig. 20 Effect of temperature on CO_2 consumption during gasification of waste tires [15]

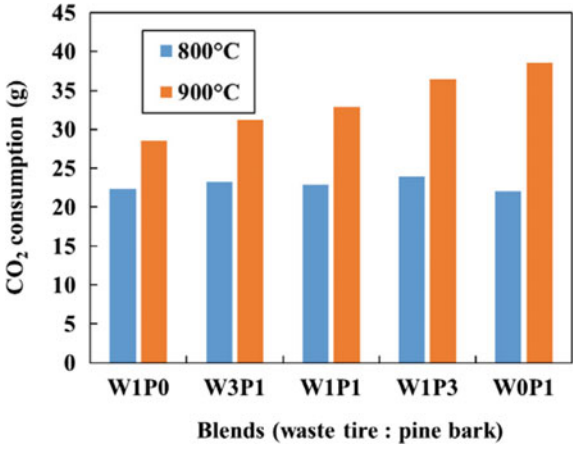

Fig. 21 Effect of feedstock blend ratio on CO_2 consumption during co-gasification of waste tires with pine bark [18]

Additionally, co-gasification also seemed to not provide any non-additive behavior and was similarly superimposable as the syngas yields from co-gasification.

These studies provide important pathways that establish the capability of thermochemical pathways of pyrolysis and CO_2-assisted gasification for efficient, sustainable and economic recovery of waste tires to energy.

6 Conclusions

This chapter provides improved understanding for efficient disposal of real waste tires via thermochemical pathways such as pyrolysis and CO_2-assisted gasification in return for syngas which provides with versatility in utilization and uniformity in handling. Syngas obtained from this pathway is useful for various applications including use as fuel for energy recovery and value-added chemicals production such as methanol, and Fischer–Tropsch transportation fuels. Thermogravimetric analysis revealed the waste tire samples to thermally decompose between temperatures of 120–550 °C and included mass-loss rate peaks of different elastomer content and the additives such as extender oils. Curve-fitting this data with TGA results from straight-chain elastomers of similar nature to those present in the examined waste tire revealed the composition to be dominated by butadiene and styrene–butadiene rubbers, while natural rubber's contribution was only about 5%. Pyrolysis and gasification were carried out using a lab-scale fixed bed reactor to understand the evolution, yield and composition of the product gases extracted. Temperature had significant influence on the syngas yield and composition, where high temperatures led to increased syngas. Endothermic reactions such as thermal cracking of volatile intermediates released from waste tire pyrolysis, CO_2-reforming of the hydrocarbons into H_2 and CO, and Boudouard reaction of CO_2 with char residue were enhanced on both equilibrium and kinetic front to increase the yield and lead to faster release of syngas. Waste tire's char poses a difficulty in gasification as the CO yield from its conversion was low and continued for extended periods of time that concluded low reactivity of its chars. BET surface area value of char from waste tire was only about a half of that from pine bark char. Co-pyrolysis and co-gasification of waste tire and pine bark biomass were also conducted in various proportions of their blends. The results revealed almost no synergistic or inhibitive interaction between waste tire conversion and pine bark conversion, and the results obtained were found to be a weighted superimposition of the results from their respective conversions when conducted separately. These results are a step closer to developing feed-flexible gasifiers that can provide with sustained syngas output and efficiency from various feedstocks with minimal changes to its operating conditions. The lack of any inhibitive interactions means that waste tire can be co-processed with pine bark or vice versa, and the predictable behavior allows one for easier designing of the reactor, while the feedstock can be adjusted to maintain the energy input and other design parameters.

Overall energy efficiency was also calculated for these processes based on the syngas's calorific content, the measured electrical energy requirements for the lab-scale reactors and the calorific content of the feedstock. The results revealed efficiency to improve with increase in temperature that reached as high as 38% in pyrolysis and 30% in CO_2-assisted gasification wherein higher unreformed hydrocarbons in pyrolysis products and their high heating value compared to reformed CO from gasification led to this differences. Incorporating char energy from the measured heating values of the chars to the overall energy efficiency resulted in efficiency to reach almost 50%. Additionally, the co-processing of waste tire with pine bark was able to provide a cumulative synergistic enhancement in efficiency beyond the weighted efficiency that could be achieved by separate conversion of the two components. These results establish the feasibility of pyrolysis and CO_2-assisted gasification of waste tire and its mixtures with biomass as sustainable pathway for their disposal while providing usable syngas.

A major challenge for future studies into these pathways is the waste tire char that was found to be of low reactivity and surface area while being a significant by-product that accounted for almost 30% of the sample mass. Developing pathway for conversion and utilization of this char is essential to not only make these pathways sustainable and efficient in material management, but also to provide economic support. Future research needs to focus on producing high-value carbon products from these char residues, such as carbon catalysts, activated carbon for sorption, electrochemical and energy storage applications to replace expensive materials (such as synthetic graphite and fossil fuel-derived activated carbon), high-quality solid fuel, and carbon dots for biomedical and other imaging applications. These activities will help provide improved value to economically support the thermochemical pathways so that waste tires can be disposed in an eco-friendly fashion while sustainably recovering energy and producing value-added chemicals.

Acknowledgements This work was supported by Office of Naval Research (ONR), and it is gratefully acknowledged. K. G. Burra received Ann. G Wylie fellowship, and this support is gratefully acknowledged.

References

1. Keeling R (2020) Scripps institute of oceanography 2020. https://scrippsco2.ucsd.edu/. Accessed 26 Sep 2020
2. Association U tire rubber. 2017 U. S. scrap tire management summary about the U. S. Tire Manufacturers Association 2018
3. Machin EB, Pedroso DT, de Carvalho JA (2017) Energetic valorization of waste tires. Renew Sustain Energy Rev 68:306–315. https://doi.org/10.1016/j.rser.2016.09.110
4. Wang Z, Burra KG, Zhang M, Li X, Policella M, Lei T et al (2020) Co-pyrolysis of waste tire and pine bark for syngas and char production. Fuel 274:117878. https://doi.org/10.1016/j.fuel.2020.117878

5. Martínez JD, Puy N, Murillo R, García T, Navarro MV, Mastral AM (2013) Waste tyre pyrolysis—a review. Renew Sustain Energy Rev 23:179–213. https://doi.org/10.1016/j.rser.2013.02.038
6. Burra KG, Gupta AK (2018) Thermochemical reforming of wastes to renewable fuels. In: Runchal AK, Gupta AK, Kushari A, De A, Aggarwal SK (eds) Energy propuls. A sustain. Technol. Approach, Springer, Singapore, pp 395–428. https://doi.org/10.1007/978-981-10-7473-8_17
7. Hasan A, Dincer I (2019) Comparative assessment of various gasification fuels with waste tires for hydrogen production. Int J Hydrogen Energy 44:18818–18826. https://doi.org/10.1016/j.ijhydene.2018.11.150
8. González JF, Encinar JM, Canito JL, Rodríguez JJ (2001) Pyrolysis of automobile tyre waste. Influence of operating variables and kinetics study. J Anal Appl Pyrolysis 58–59:667–83. https://doi.org/10.1016/S0165-2370(00)00201-1
9. Colom X, Faliq A, Formela K, Cañavate J (2016) FTIR spectroscopic and thermogravimetric characterization of ground tyre rubber devulcanized by microwave treatment. Polym Test 52:200–208. https://doi.org/10.1016/j.polymertesting.2016.04.020
10. Banar M, Akyıldız V, Özkan A, Çokaygil Z, Onay Ö (2012) Characterization of pyrolytic oil obtained from pyrolysis of TDF (Tire Derived Fuel). Energy Convers Manag 62:22–30. https://doi.org/10.1016/j.enconman.2012.03.019
11. Kar Y (2011) Catalytic pyrolysis of car tire waste using expanded perlite. Waste Manag 31:1772–1782. https://doi.org/10.1016/j.wasman.2011.04.005
12. Cunliffe AM, Williams PT (1998) Composition of oils derived from the batch pyrolysis of tyres. J Anal Appl Pyrolysis 44:131–152. https://doi.org/10.1016/S0165-2370(97)00085-5
13. Karatas H, Olgun H, Engin B, Akgun F (2013) Experimental results of gasification of waste tire with air in a bubbling fluidized bed gasifier. Fuel 105:566–571. https://doi.org/10.1016/j.fuel.2012.08.038
14. Williams PT (2013) Pyrolysis of waste tyres: a review. Waste Manag 33:1714–1728. https://doi.org/10.1016/j.wasman.2013.05.003
15. Policella M, Wang Z, Burra KG, Gupta AK (2019) Characteristics of syngas from pyrolysis and CO_2-assisted gasification of waste tires. Appl Energy 254:113678. https://doi.org/10.1016/j.apenergy.2019.113678
16. Oboirien BO, North BC (2017) A review of waste tyre gasification. J Environ Chem Eng 5:5169–5178. https://doi.org/10.1016/j.jece.2017.09.057
17. Ucar S, Karagoz S, Ozkan AR, Yanik J (2005) Evaluation of two different scrap tires as hydrocarbon source by pyrolysis. Fuel 84:1884–1892. https://doi.org/10.1016/j.fuel.2005.04.002
18. Wang Z, Burra KG, Lei T, Gupta AK (2019) Co-gasification characteristics of waste tire and pine bark mixtures in CO_2 atmosphere. Fuel 257:116025. https://doi.org/10.1016/j.fuel.2019.116025
19. Williams PT, Besler S, Taylor DT (1990) The pyrolysis of scrap automotive tyres. Fuel 69:1474–1482. https://doi.org/10.1016/0016-2361(90)90193-T
20. Portofino S, Donatelli A, Iovane P, Innella C, Civita R, Martino M et al (2013) Steam gasification of waste tyre: influence of process temperature on yield and product composition. Waste Manag 33:672–678. https://doi.org/10.1016/j.wasman.2012.05.041
21. Rofiqulislam M, Haniu H, Rafiqulalambeg M (2008) Liquid fuels and chemicals from pyrolysis of motorcycle tire waste: product yields, compositions and related properties. Fuel 87:3112–3122. https://doi.org/10.1016/j.fuel.2008.04.036
22. Chen DT, Perman CA, Riechert ME, Hoven J (1995) Depolymerization of tire and natural rubber using supercritical fluids. J Hazard Mater 44:53–60. https://doi.org/10.1016/0304-3894(95)00047-X
23. Lah B, Klinar D, Likozar B (2013) Pyrolysis of natural, butadiene, styrene-butadiene rubber and tyre components: modelling kinetics and transport phenomena at different heating rates and formulations. Chem Eng Sci 87:1–13. https://doi.org/10.1016/j.ces.2012.10.003

24. Berrueco C, Esperanza E, Mastral FJ, Ceamanos J, García-Bacaicoa P (2005) Pyrolysis of waste tyres in an atmospheric static-bed batch reactor: analysis of the gases obtained. J Anal Appl Pyrolysis 74:245–253. https://doi.org/10.1016/j.jaap.2004.10.007
25. Xiao G, Ni M-J, Chi Y, Cen K-F (2008) Low-temperature gasification of waste tire in a fluidized bed. Energy Convers Manag 49:2078–2082. https://doi.org/10.1016/j.enconman.2008.02.016
26. Conesa JA, Martín-Gullón I, Font R, Jauhiainen J (2004) Complete study of the pyrolysis and gasification of scrap tires in a pilot plant reactor. Environ Sci Technol 38:3189–3194. https://doi.org/10.1021/es034608u
27. de Marco RI, Laresgoiti M, Cabrero M, Torres A, Chomón M, Caballero B (2001) Pyrolysis of scrap tyres. Fuel Process Technol 72:9–22. https://doi.org/10.1016/S0378-3820(01)00174-6
28. Kim S, Park JK, Chun H-D (1995) Pyrolysis kinetics of scrap tire rubbers. I: Using DTG and TGA. J Environ Eng 121:507–14. https://doi.org/10.1061/(ASCE)0733-9372(1995)121:7(507)
29. Zabaniotou A, Stavropoulos G (2003) Pyrolysis of used automobile tires and residual char utilization. J Anal Appl Pyrolysis 70:711–722. https://doi.org/10.1016/S0165-2370(03)00042-1
30. Evans A, Evans R (2006) The composition of a tyre: typical components. Waste Resour Action Program 2006. http://www.wrap.org.uk/sites/files/wrap/2 - Composition of a Tyre - May 2006.pdf=https://doi.org/10.3233/HAB-1993-4306
31. Aylón E, Fernández-Colino A, Murillo R, Navarro MV, García T, Mastral AM (2010) Valorisation of waste tyre by pyrolysis in a moving bed reactor. Waste Manag 30:1220–1224. https://doi.org/10.1016/j.wasman.2009.10.001
32. Scala F, Chirone R, Salatino P (2003) Fluidized bed combustion of tyre derived fuel. Exp Therm Fluid Sci 27:465–471. https://doi.org/10.1016/S0894-1777(02)00249-2
33. Lee JM, Lee JS, Kim JR, Kim SD (1995) Pyrolysis of waste tires with partial oxidation in a fluidized-bed reactor. Energy 20:969–976. https://doi.org/10.1016/0360-5442(95)00049-M
34. Chang YM (1996) On pyrolysis of waste tire: degradation rate and product yields. Resour Conserv Recycl 17:125–139. https://doi.org/10.1016/0921-3449(96)01059-2
35. Dai X, Yin X, Wu C, Zhang W, Chen Y (2001) Pyrolysis of waste tires in a circulating fluidized-bed reactor. Energy 26:385–399. https://doi.org/10.1016/S0360-5442(01)00003-2
36. Leung DYC, Yin XL, Zhao ZL, Xu BY, Chen Y (2002) Pyrolysis of tire powder: influence of operation variables on the composition and yields of gaseous product. Fuel Process Technol 79:141–155. https://doi.org/10.1016/S0378-3820(02)00109-1
37. Li S-Q, Yao Q, Chi Y, Yan J-H, Cen K-F (2004) Pilot-scale pyrolysis of scrap tires in a continuous rotary kiln reactor. Ind Eng Chem Res 43:5133–5145. https://doi.org/10.1021/ie030115m
38. Roy C, Labrecque B, de Caumia B (1990) Recycling of scrap tires to oil and carbon black by vacuum pyrolysis. Resour Conserv Recycl 4:203–213. https://doi.org/10.1016/0921-3449(90)90002-L
39. Senneca O, Salatino P, Chirone R (2000) A fast heating-rate thermogravimetric study of the pyrolysis of scrap tyres. Fuel Energy Abstr 41:104. https://doi.org/10.1016/S0140-6701(00)90920-2
40. Zhang X, Wang T, Ma L, Chang J (2008) Vacuum pyrolysis of waste tires with basic additives. Waste Manag 28:2301–2310. https://doi.org/10.1016/j.wasman.2007.10.009
41. Murillo R, Aylón E, Navarro M, Callén M, Aranda A, Mastral A (2006) The application of thermal processes to valorise waste tyre. Fuel Process Technol 87:143–147. https://doi.org/10.1016/j.fuproc.2005.07.005
42. Larsen MB, Schultz L, Glarborg P, Skaarup-Jensen L, Dam-Johansen K, Frandsen F et al (2006) Devolatilization characteristics of large particles of tyre rubber under combustion conditions. Fuel 85:1335–1345. https://doi.org/10.1016/j.fuel.2005.12.014
43. López FA, Centeno TA, Alguacil FJ, Lobato B (2011) Distillation of granulated scrap tires in a pilot plant. J Hazard Mater 190:285–292. https://doi.org/10.1016/j.jhazmat.2011.03.039
44. Betancur M, Daniel Martínez J, Murillo R (2009) Production of activated carbon by waste tire thermochemical degradation with CO_2. J Hazard Mater 168:882–887. https://doi.org/10.1016/j.jhazmat.2009.02.167

45. Díez C, Martínez O, Calvo LF, Cara J, Morán A (2004) Pyrolysis of tyres. Influence of the final temperature of the process on emissions and the calorific value of the products recovered. Waste Manag 24:463–9. https://doi.org/10.1016/j.wasman.2003.11.006
46. Aydın H, İlkılıç C (2012) Optimization of fuel production from waste vehicle tires by pyrolysis and resembling to diesel fuel by various desulfurization methods. Fuel 102:605–612. https://doi.org/10.1016/j.fuel.2012.06.067
47. Williams PT, Bottrill RP, Cunliffe AM (1998) Combustion of tyre pyrolysis oil. Process Saf Environ Prot 76:291–301. https://doi.org/10.1205/095758298529650
48. Laresgoiti M, Caballero B, de Marco I, Torres A, Cabrero M, Chomón M (2004) Characterization of the liquid products obtained in tyre pyrolysis. J Anal Appl Pyrolysis 71:917–934. https://doi.org/10.1016/j.jaap.2003.12.003
49. Islam RM, Hossain Joardder MU, Kader MA, Islam Sarker MR (2011) Valorization of solid tire wastes available in Bangladesh by thermal treatment. In: Proceedings of the WasteSafe 2011—2nd international conference on solid waste management in the developing countries, Khulna, Bangladesh, pp 1–9
50. Galvagno S, Casu S, Casabianca T, Calabrese A, Cornacchia G (2002) Pyrolysis process for the treatment of scrap tyres: preliminary experimental results. Waste Manag 22:917–923. https://doi.org/10.1016/S0956-053X(02)00083-1
51. Kaminsky W, Mennerich C, Zhang Z (2009) Feedstock recycling of synthetic and natural rubber by pyrolysis in a fluidized bed. J Anal Appl Pyrolysis 85:334–337. https://doi.org/10.1016/j.jaap.2008.11.012
52. Williams PT, Brindle AJ (2003) Fluidised bed pyrolysis and catalytic pyrolysis of scrap tyres. Environ Technol 24:921–929. https://doi.org/10.1080/09593330309385629
53. Olazar M, Aguado R, Arabiourrutia M, Lopez G, Barona A, Bilbao J (2008) Catalyst effect on the composition of tire pyrolysis products. Energy Fuels 22:2909–2916. https://doi.org/10.1021/ef8002153
54. Lopez G, Olazar M, Aguado R, Elordi G, Amutio M, Artetxe M et al (2010) Vacuum pyrolysis of waste tires by continuously feeding into a conical spouted bed reactor. Ind Eng Chem Res 49:8990–8997. https://doi.org/10.1021/ie1000604
55. Roy C, Chaala A, Darmstadt H (1999) The vacuum pyrolysis of used tires. J Anal Appl Pyrolysis 51:201–221. https://doi.org/10.1016/S0165-2370(99)00017-0
56. Pakdel H, Pantea DM, Roy C (2001) Production of dl-limonene by vacuum pyrolysis of used tires. J Anal Appl Pyrolysis 57:91–107. https://doi.org/10.1016/S0165-2370(00)00136-4
57. Miranda M, Pinto F, Gulyurtlu I, Cabrita I (2013) Pyrolysis of rubber tyre wastes: a kinetic study. Fuel 103:542–552. https://doi.org/10.1016/j.fuel.2012.06.114
58. Murugan S, Ramaswamy MC, Nagarajan G (2008) The use of tyre pyrolysis oil in diesel engines. Waste Manag 28:2743–2749. https://doi.org/10.1016/j.wasman.2008.03.007
59. Harker JH, Backhurst JR (1981) Fuel and energy
60. Wieckert C, Obrist A, Von ZP, Maag G, Steinfeld A (2013) Syngas production by thermochemical gasification of carbonaceous waste materials in a 150 kW th packed-bed solar reactor. Energy Fuels 27:4770–4776. https://doi.org/10.1021/ef4008399
61. Pattabhi Raman K, Walawender WP, Fan LT (1981) Gasification of waste tires in a fluid bed reactor. Conserv Recycl 4:79–88. https://doi.org/10.1016/0361-3658(81)90036-9
62. Donatelli A, Iovane P, Molino A (2010) High energy syngas production by waste tyres steam gasification in a rotary kiln pilot plant. Experimental and numerical investigations. Fuel 89:2721–2728. https://doi.org/10.1016/j.fuel.2010.03.040
63. Zhang Y, Wu C, Nahil MA, Williams P (2015) Pyrolysis-catalytic reforming/gasification of waste tires for production of carbon nanotubes and hydrogen. Energy Fuels 29:3328–3334. https://doi.org/10.1021/acs.energyfuels.5b00408
64. Lerner AS, Bratsev AN, Popov VE, Kuznetsov VA, Ufimtsev AA, Shengel' SV et al (2012) Production of hydrogen-containing gas using the process of steam-plasma gasification of used tires. Glas Phys Chem 38:511–6. https://doi.org/10.1134/S1087659612060041
65. Burra KG, Gupta AK (2018) Synergistic effects in steam gasification of combined biomass and plastic waste mixtures. Appl Energy 211:230–236. https://doi.org/10.1016/j.apenergy.2017.10.130

66. Wu Z, Yang W, Tian X, Yang B (2017) Synergistic effects from co-pyrolysis of low-rank coal and model components of microalgae biomass. doi:https://doi.org/10.1016/j.enconman.2016.12.060
67. Zhang Y, Geng P, Liu R (2018) Synergistic combination of biomass torrefaction and co-gasification: Reactivity studies. Bioresour Technol 245:225–233. https://doi.org/10.1016/j.biortech.2017.08.197
68. Chen W, Shi S, Zhang J, Chen M, Zhou X (2016) Co-pyrolysis of waste newspaper with high-density polyethylene: synergistic effect and oil characterization. Energy Convers Manag 112:41–48. https://doi.org/10.1016/j.enconman.2016.01.005
69. Déparrois N, Singh P, Burra KG, Gupta AK (2019) Syngas production from co-pyrolysis and co-gasification of polystyrene and paper with CO_2. Appl Energy 246:1–10. https://doi.org/10.1016/j.apenergy.2019.04.013
70. Ahmed II, Nipattummakul N, Gupta AK (2011) Characteristics of syngas from co-gasification of polyethylene and woodchips. Appl Energy 88:165–174. https://doi.org/10.1016/j.apenergy.2010.07.007